*Mon. Not. R. astr. Soc.* (1966) **133**, 359–387.

# A NEUTRAL HYDROGEN SURVEY OF THE SOUTHERN REGIONS OF THE ANDROMEDA NEBULA

*S. T. Gottesman, R. D. Davies and V. C. Reddish**

(Received 1965 October 22)

*Summary*

A neutral hydrogen survey of the southern region of M 31 and selected regions in the north including the major axis has been made with a beamwidth of 15′ and a bandwidth of 200 kc/s (42 km/s). Neutral hydrogen was found out to 150′ from the centre along the major axis. A major concentration in the neutral hydrogen distribution was observed in a broad ring of radius 9 kpc. Within 120′ from the centre the neutral hydrogen concentrations coincide with the major H II features. The overall neutral hydrogen mass was estimated to be $2{\cdot}4 \times 10^9 M_\odot$ at a distance of 630 kpc while the ionized hydrogen mass was calculated to be less than $1{\cdot}5 \times 10^7 M_\odot$.

A new rotation curve has been obtained for M 31. It shows apparently significant differences between the NE and SW sections. The mean rotation curve indicates a mass of $2{\cdot}4 \times 10^{11} M_\odot$ out to 150′ and an estimated total mass of $4{\cdot}8 \times 10^{11} M_\odot$. The mass distribution determined from the rotation curve shows a less strong central concentration than Schmidt obtained from the van de Hulst, Raimond & van Woerden data. The $M/L_B$ distribution uncorrected for obscuration shows a constant value of $\sim 20$ between 30′ and 75′ from the centre. The mean value of $M/L_B$ taken out to 120′ is $\sim 16$ which on correction for obscuration is $\sim 9$.

1. *Introduction.* Previous neutral hydrogen studies of the Andromeda nebula (M 31) have indicated a broad distribution of gas relative to stars. Investigations so far have been restricted either to observations along the major and minor axes of the nebula (van de Hulst, Raimond & van Woerden 1957, Burke, Turner & Tuve 1964) or to observations of the whole nebula with a relatively broad (36′) beamshape (Argyle 1965).

The present investigation is aimed at surveying in detail a significant fraction of M 31 with the narrow beam of the 250 ft radio telescope. Because of the large number of data points contained in the frequency and position domains of the nebula the first observations were limited mainly to declinations south of 41°36′ with additional scans along the major axis. A relatively coarse frequency resolution of 200 kc/s was used. The next stage of the investigation now in progress is the survey of the entire nebula with a frequency resolution of 50 kc/s.

The observations described here enable the neutral hydrogen distribution to be compared with the optical features of the nebula. Moreover, a reliable rotation curve not greatly affected by angular resolution can be obtained from which a model of the mass distribution in M 31 is derived.

2. *Observational technique and reductions.* The beamwidth of the 250 ft radio telescope illuminated by a dipole and shaped reflecting plate at the focus of the

* Now at the Royal Edinburgh Observatory.

main reflector was 18′ in the elevation plane and 12′ in the azimuth plane; this illumination gave minimum power in the nearby sidelobes.

The receiver used for the observations which were undertaken in the period 1961 April to 1961 June was a mixer with a system noise of about 1 000 °K which had a single receiving band 200 kc/s wide. A d.c. comparison system was employed in which a 1 Mc/s bandwidth channel displaced 5 Mc/s from the hydrogen line frequency is detected and continuously subtracted from the detected output of the 200 kc/s bandwidth hydrogen line channel. With a 20 s time constant the r.m.s. noise was 0·45 °K which corresponded to 1·0 °K of brightness temperature in the nebula.

The observing technique consisted of making drift scans in right ascension across M 31 at fixed frequencies so that full information was obtained in angle with the best positional accuracy obtainable using the azimuth–elevation position indicators. Drifts covered $15^m$ in right ascension centred on the major axis of the nebula at each declination and were thus sufficiently long to obtain a good zero level each side of the nebula free from neutral hydrogen emission. The drifts were repeated at least twice and in most cases three times at each frequency to improve the signal to noise ratio of the results.

The temperature calibration was made daily by comparing the observed drifts with scans taken at a fixed frequency across the galactic plane at $l^{\mathrm{I}} = 90°$ between $b^{\mathrm{I}} = +10°$ and $-10°$. These measurements were necessary to account for the broad outer sidelobes of the 250 ft radio telescope which extend to 2·5° from the main beam at the 30 db level. The observations at $l^{\mathrm{I}} = 90°$ were then compared with the Kootwijk spectra (Westerhout & Muller 1957) which were smoothed with a 200 kc/s bandwidth. Angular smoothing was also necessary to take account of the difference in beamwidth between the Kootwijk and Jodrell Bank aerials.

After the individual drifts at each frequency had been averaged and converted to brightness temperature it was necessary to remove the effect of the broad sidelobes. The maximum corrections were 10%. The resolution of the survey can be taken as approximately 15′ since drift curves at any particular declination were taken at a number of position angles of the elliptical beam.

The accuracy of the frequency determination was checked daily by observations of the absorption spectrum of Cassiopeia A and was found to be ± 20 kc/s (± 4 km/s). The frequencies of the drift scans were then reduced to the local standard of rest (l.s.r.) in the solar vicinity. To obtain velocities in M 31 relative to the Sun and to the centre of the Galaxy, −4 km/s and +200 km/s respectively must be added to the values given here.

3. *The results of the survey.* The major part of the survey consisted of drift scans on frequencies where neutral hydrogen emission occurred at declination south of 41°36′ (1950 coordinates). Observations were made at $\delta = 41°36'$ 41°24′, 41°12′, 41°00′, 39°50′, 39°40′, 39°30′, 39°20′, 39°00′, 38°30′, and 38°00 Additional drift scans were made $\delta = 43°00'$ and 42°30′ in the northern part c M 31. Major axis scans were also taken so that a rotation curve could be derive At each declination the average frequency separation of the scans was 200 kc/

The quality of the observational data is illustrated in Figs. 1(*a*) and (*b*) whic show the corrected drift scans obtained at $\delta = 41°00'$ and $\delta = 41°36'$ (1950.c They give the brightness temperature as a function of the right ascension relati

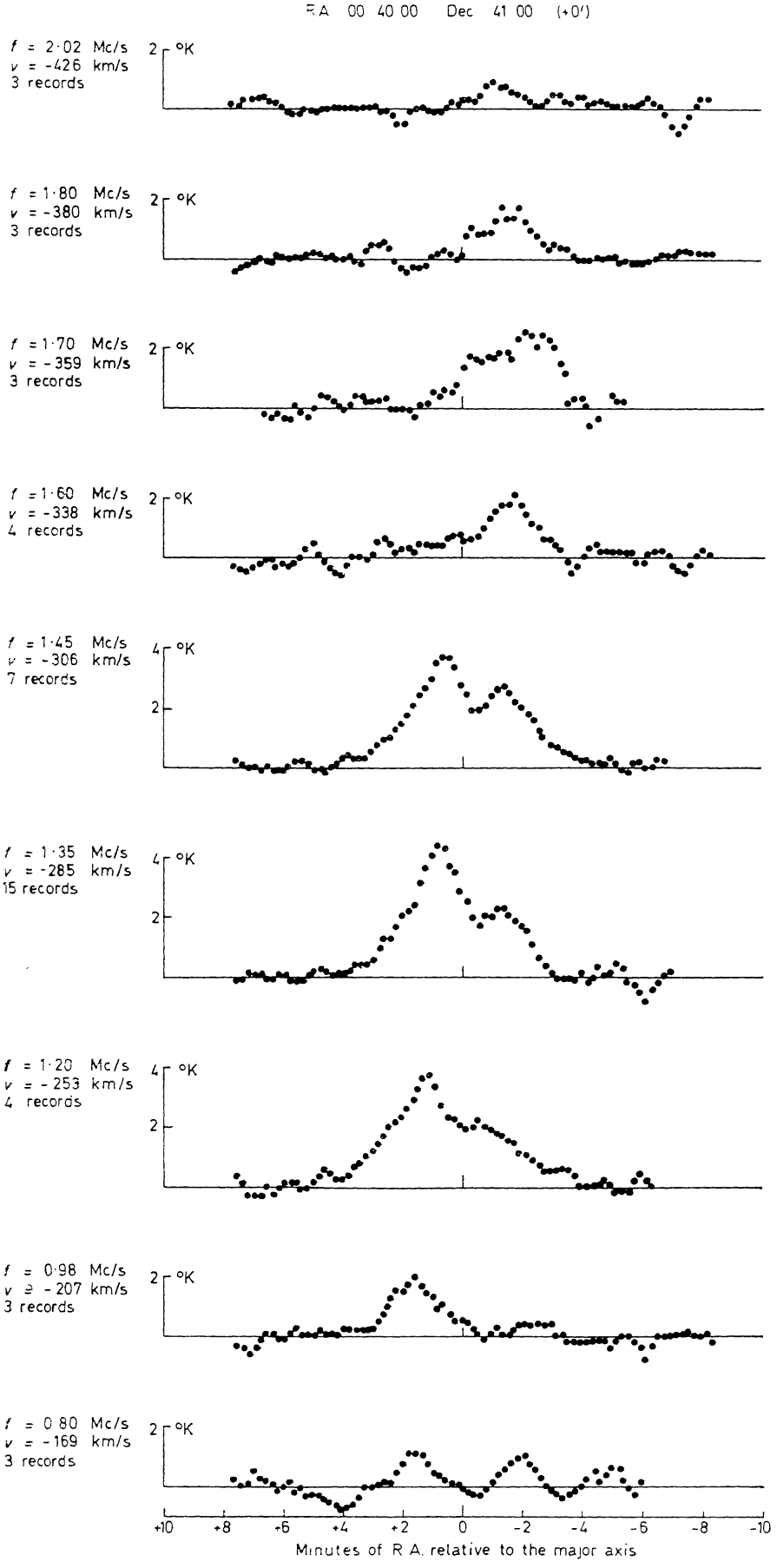


FIG. 1 (*a*).

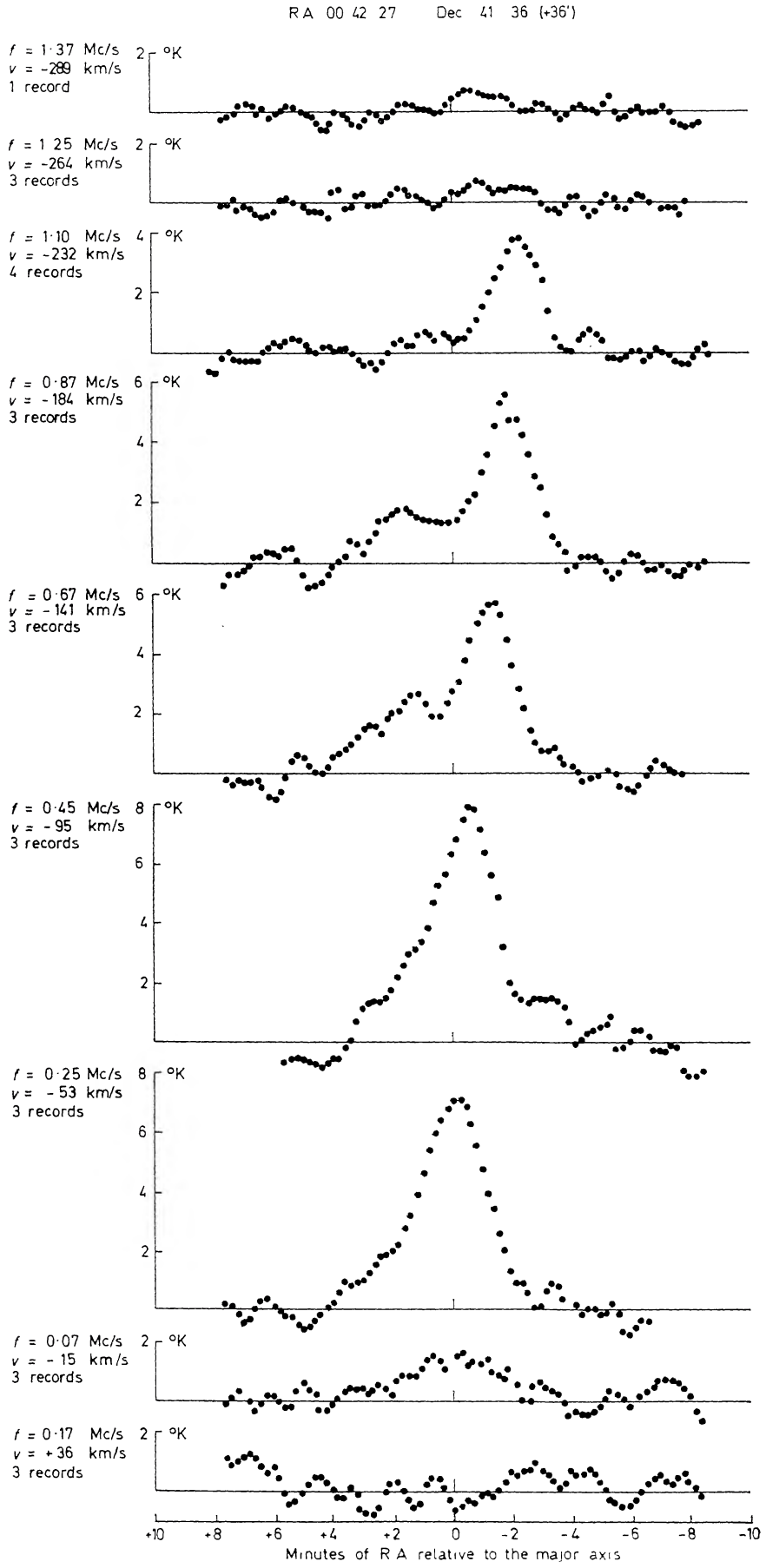


FIG. 1 (*b*).

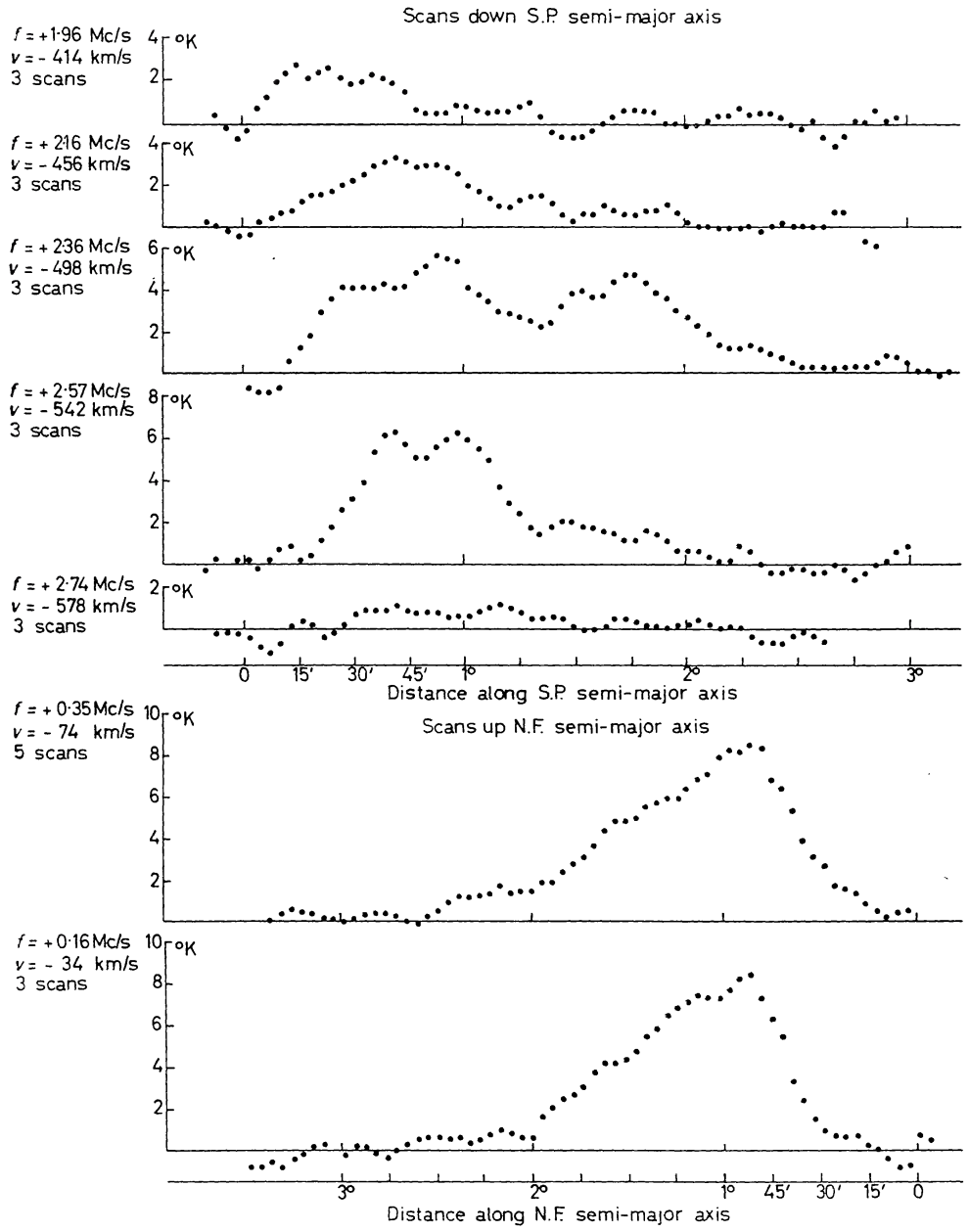


FIG. 1(*c*).

FIG. 1. *R.A. drift curves across M* 31. *The brightness temperature is plotted against R.A. relative to the intersection of the scan with the major axis. The number of records and the frequency and velocity relative to the l.s.r. are given for each drift curve.* (*a*) *Drifts at* $\delta = 41°00'$ (1950.0). (*b*) *Drifts at* $\delta = 41°36'$ (1950.0). (*c*) *Scans along the major axis of M* 31. *The brightness temperature is plotted against distance along the major axis. The number of records and the frequency and velocity relative to the l.s.r. are given for each drift curve.*

to the intersection of the drifts with the major axis. The major axis is assumed to pass through the centre of M 31 ($\alpha = 00° 40'.0$, $\delta = 41°00'$, 1950.0 coordinates) at position angle 38° (de Vaucouleurs 1958). On each scan are shown the declination, the frequency and velocity relative to the l.s.r. and the number of scans taken to obtain the average. The scans made along the major axis are presented in Fig. 1(*c*).

Spectra have been constructed from all the drift curves (copies of all the drift curves and spectra are available upon request from Jodrell Bank). In the

declination range 41°36′ to 42°30′ a limited number of major axis scans were available and these were used to indicate the shape of the spectra in this region. Spectra for the major and minor axes are plotted in Fig. 2; those derived from limited data between declinations 41°36′ and 42°30′ are shown by dashed curves in Fig. 2 and by an asterisk in Table I. The values of the mean velocity and frequency relative to the l.s.r. and of the surface density of neutral hydrogen for each spectrum are given in Table I. Alternative interpretations of the observed spectra at the limits of the likely errors are sometimes possible and these are given in brackets in the table.

An overall picture of the variation of the shapes and intensities of spectra within M 31 is shown in Fig. 3. Spectra with double maxima can be seen in

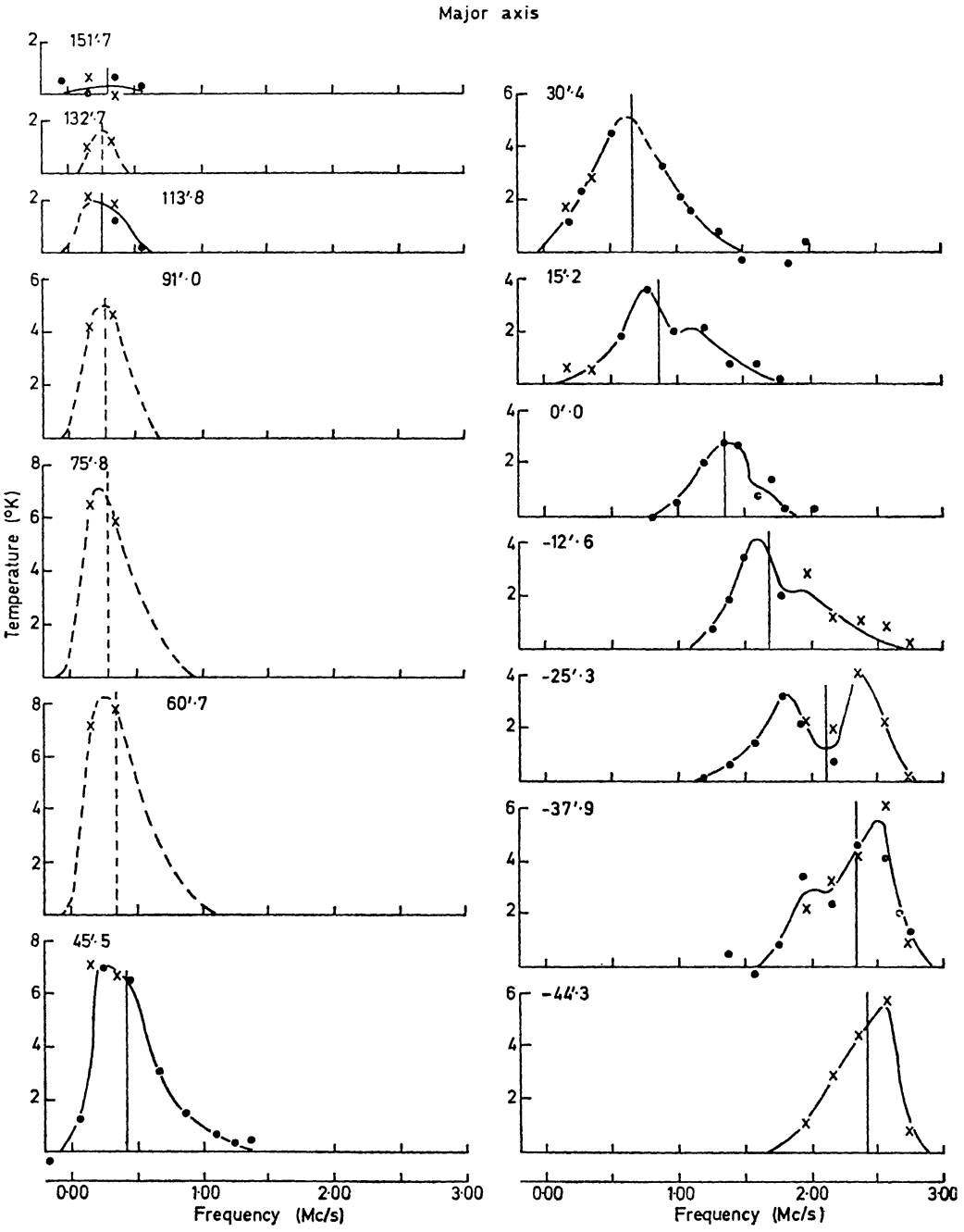


FIG. 2 (*a*).

the inner areas of M 31. The major axis scans showed a feature at $\delta = 40°40'$ on frequencies not covered by the drift scans at this declination. The other spectra at $\delta = 40°40'$ derived from drift curves only were believed to be incomplete and the data was augmented by extrapolation between adjacent declinations.

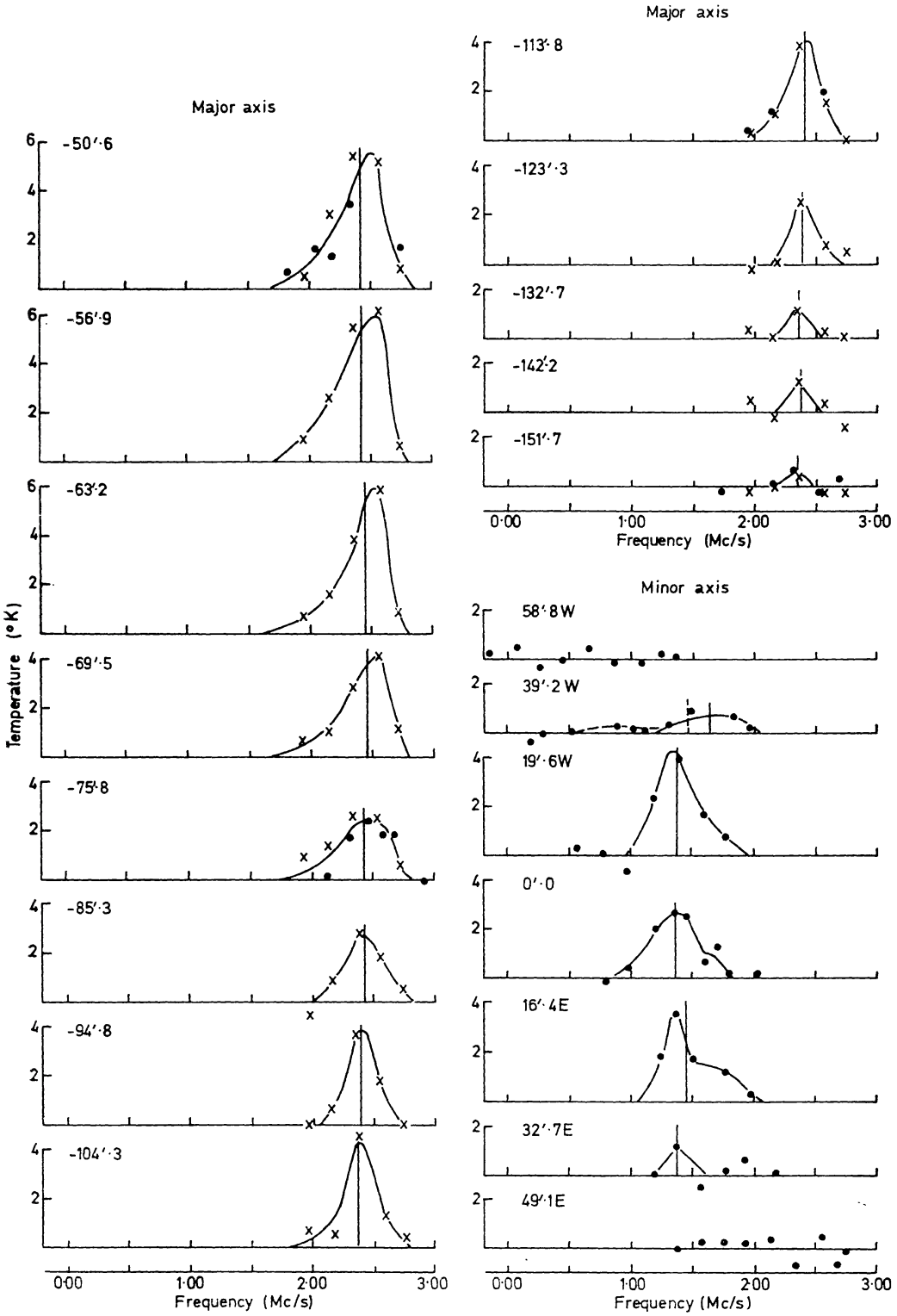


FIG. 2 (*b*).

FIG. 2 (*a*) *and* (*b*). *Spectra obtained along the major and minor axes of M* 31. *The position in terms of the major–minor axis coordinate system and the frequency relative to the l.s.r. is given for each spectrum.* (●) *Data from drift curves;* (×) *data from major axis scans.*

TABLE I

*Mean frequency and velocity of neutral hydrogen at positions X, Y in M 31. The observed surface density of neutral hydrogen $N_H$ is also tabulated.*

| $Y$ | $X$ | Frequency displacement (Mc/s) | Velocity (km/s) | $N_H$ ($10^{21}$ cm$^{-2}$) |
|---|---|---|---|---|
| *Major axis* | | | | |
| 151·7 | 0·0 | +0·30 | −63 | 0·054 |
| 132·7* | 0·0 | +0·26 | −55 | 0·155 |
| 113·4 | 0·0 | +0·25 | −53 | 0·303 |
| 91·0* | 0·0 | +0·28 | −59 | 0·815 |
| 75·8* | 0·0 | +0·30 | −63 | 1·26 |
| 60·7* | 0·0 | +0·36 | −76 | 1·65 |
| 45·5 | 0·0 | +0·42 | −89 | 1·54 |
| 30·4 | 0·0 | +0·65 | −137 | 1·35 |
| 15·2 | 0·0 | +0·86 | −181 | 0·869 |
| 0·0 | 0·0 | +1·36 | −287 | 0·528 |
| −12·6 | 0·0 | +1·68 | −354 | 1·00 |
| −25·3 | 0·0 | +2·11 | −445 | 1·16 |
| −37·9 | 0·0 | +2·34 | −494 | 1·30 |
| −44·3 | 0·0 | +2·42 | −511 | 1·13 |
| −50·6 | 0·0 | +2·41 | −508 | 1·00 |
| −56·9 | 0·0 | +2·42 | −511 | 1·11 |
| −63·2 | 0·0 | +2·45 | −517 | 0·970 |
| −69·5 | 0·0 | +2·47 | −521 | 0·698 |
| −75·8 | 0·0 | +2·43 | −513 | 0·512 |
| −85·3 | 0·0 | +2·42 | −511 | 0·435 |
| −94·8 | 0·0 | +2·39 | −504 | 0·489 |
| −104·3 | 0·0 | +2·37 | −500 | 0·574 |
| −113·8 | 0·0 | +2·40 | −506 | 0·520 |
| −123·3 | 0·0 | +2·39 | −504 | 0·248 |
| −132·7 | 0·0 | +2·36 | −498 | 0·093 |
| −142·2 | 0·0 | +2·37 | −500 | 0·078 |
| −151·7 | 0·0 | +2·35 | −496 | 0·047 |
| *Minor axis* | | | | |
| 0·0 | 58·8 W | ... | ... | ... |
| 0·0 | 39·2 W | (+1·84)<br>+1·46 | (−388)<br>−308 | (0·163)<br>0·217 |
| 0·0 | 19·6 W | +1·38 | −292 | 0·683 |
| 0·0 | 0·0 | +1·36 | −287 | 0·528 |
| 0·0 | 16·4 E | +1·44 | −304 | 0·559 |
| 0·0 | 32·7 E | +1·38 | −291 | 0·109 |
| 0·0 | 49·1 E | ... | ... | ... |
| *Off axis positions* | | | | |
| 155·2 | 4·5 E | +0·56 | −118 | 0·070 |
| 117·3 | 4·5 E | (+0·36)<br>+0·27 | (−76)<br>−57 | (0·047)<br>0·124 |
| 49·0 | 4·5 E | +0·40 | −84 | 1·30 |
| 33·9 | 4·5 E | +0·66 | −139 | 1·27 |
| 18·7 | 4·5 E | +0·94 | −198 | 1·23 |
| 3·5 | 4·5 E | +1·33 | −281 | 0·667 |
| −9·1 | 4·5 E | (+1·54)<br>+1·62 | (−325)<br>−342 | (0·722)<br>0·931 |

TABLE I (*continued*)

| $Y$ | $X$ | Frequency displacement (Mc/s) | Velocity (km/s) | $N_H$ ($10^{21}$ cm$^{-2}$) |
|---|---|---|---|---|
| −21·8 | 4·5 E | (+1·70) | (−371) | (0·931) |
| | | +1·86 | −392 | 1·23 |
| −34·4 | 4·5 E | +2·25 | −475 | 1·01 |
| −47·0 | 4·5 E | +2·46 | −519 | 1·16 |
| −72·3 | 4·5 E | +2·57 | −530 | 0·473 |
| −110·3 | 4·5 E | +2·38 | −502 | 0·528 |
| −148·2 | 4·5 E | +2·34 | −494 | 0·047 |
| 157·8 | 8·9 E | +0·56 | −118 | 0·039 |
| 120·7 | 8·9 E | ... | ... | ... |
| 52·4 | 8·9 E | +0·46 | −97 | 1·07 |
| 37·3 | 8·9 E | +0·70 | −148 | 0·908 |
| 22·1 | 8·9 E | +0·88 | −186 | 1·24 |
| 6·9 | 8·9 E | +1·28 | −270 | 0·776 |
| −5·7 | 8·9 E | +1·54 | −325 | 0·753 |
| −18·4 | 8·9 E | +1·74 | −367 | 1·02 |
| −31·0 | 8·9 E | +2·11 | −445 | 0·729 |
| −43·7 | 8·9 E | +2·40 | −506 | 1·063 |
| −69·0 | 8·9 E | +2·42 | −511 | 0·528 |
| −106·9 | 8·9 E | +2·30 | −485 | 0·551 |
| −144·8 | 8·9 E | +2·20 | −464 | 0·124 |
| 161·4 | 12·5 E | ... | ... | ... |
| 123·5 | 12·5 E | ... | ... | ... |
| 55·2 | 12·5 E | +0·51 | −108 | 1·02 |
| 40·1 | 12·5 E | +0·76 | −160 | 0·760 |
| 24·9 | 12·5 E | +0·85 | −179 | 1·15 |
| 9·7 | 12·5 E | +1·20 | −253 | 0·737 |
| −2·9 | 12·5 E | +1·49 | −314 | 0·722 |
| −15·6 | 12·5 E | (+1·67) | (−352) | (0·970) |
| | | +1·72 | −363 | 1·12 |
| −28·2 | 12·5 E | +1·96 | −414 | 0·698 |
| −40·8 | 12·5 E | +2·37 | −500 | 0·931 |
| −66·1 | 12·5 E | +2·48 | −523 | 0·473 |
| −104·0 | 12·5 E | +2·32 | −490 | 0·435 |
| −142·0 | 12·5 E | +2·36 | −498 | 0·155 |
| 58·1 | 16·3 E | +0·54 | −114 | 0·823 |
| 43·0 | 16·3 E | +0·84 | −177 | 0·636 |
| 27·8 | 16·3 E | +0·85 | −179 | 0·760 |
| 12·6 | 16·3 E | +1·18 | −249 | 0·660 |
| 0·0 | 16·3 E | +1·44 | −304 | 0·559 |
| −12·7 | 16·3 E | +1·64 | −346 | 1·08 |
| −25·3 | 16·3 E | +1·87 | −395 | 0·605 |
| −37·9 | 16·3 E | +2·17 | −458 | 0·698 |
| −63·2 | 16·3 E | +2·46 | −519 | 0·303 |
| −101·2 | 16·3 E | +2·30 | −485 | 0·349 |
| −139·1 | 16·3 E | +2·34 | −504 | 0·186 |
| 60·7 | 19·6 E | +0·57 | −120 | 0·605 |
| 45·6 | 19·6 E | +0·90 | −190 | 0·419 |
| 30·4 | 19·6 E | +0·90 | −190 | 0·466 |
| 15·2 | 19·6 E | +1·16 | −245 | 0·481 |
| 2·6 | 19·6 E | +1·40 | −295 | 0·535 |
| −10·1 | 19·6 E | (+1·60) | (−338) | (0·792) |
| | | +1·64 | −346 | 0·916 |
| −22·7 | 19·6 E | +1·92 | −405 | 0·582 |
| −35·3 | 19·6 E | +2·08 | −439 | 0·566 |
| 2·6 | 16·2 W | +1·39 | −293 | 0·792 |

TABLE I (*continued*)

| $Y$ | $X$ | Frequency displacement (Mc/s) | Velocity (km/s) | $N_H$ ($10^{21}$ cm$^{-2}$) |
|---|---|---|---|---|
| −60·6 | 19·6 E | +2·40 | −506 | 0·279 |
| −98·5 | 19·6 E | +2·34 | −494 | 0·163 |
| −136·5 | 19·6 E | +2·43 | −513 | 0·171 |
| 62·8 | 22·4 E | +0·52 | −110 | 0·572 |
| 47·7 | 22·4 E | +0·92 | −194 | 0·372 |
| 32·5 | 22·4 E | +0·81 | −171 | 0·310 |
| 17·3 | 22·4 E | +1·23 | −260 | 0·341 |
| 4·7 | 22·4 E | +1·37 | −289 | 0·388 |
| −8·0 | 22·4 E | (+1·55) | (−327) | (0·605) |
| | | +1·63 | −344 | 0·815 |
| −20·6 | 22·4 E | +1·89 | −399 | 0·621 |
| −33·3 | 22·4 E | +2·02 | −426 | 0·419 |
| −58·6 | 22·4 E | +2·44 | −515 | 0·186 |
| −96·5 | 22·4 E | +2·10 | −443 | 0·132 |
| −134·4 | 22·4 E | +2·55 | −538 | 0·047 |
| 66·3 | 26·8 E | +0·52 | −110 | 0·357 |
| 51·1 | 26·8 E | +0·96 | −203 | 0·178 |
| 35·9 | 26·8 E | +0·90 | −190 | 0·318 |
| 20·8 | 26·8 E | +1·24 | −262 | 0·124 |
| 8·1 | 26·8 E | +1·30 | −274 | 0·194 |
| −4·5 | 26·8 E | (+1·43) | (−302) | (0·233) |
| | | +1·55 | −327 | 0·341 |
| −17·2 | 26·8 E | +1·90 | −401 | 0·473 |
| −29·8 | 26·8 E | +1·89 | −399 | 0·318 |
| −55·1 | 26·8 E | +2·45 | −517 | 0·124 |
| −93·0 | 26·8 E | ... | ... | ... |
| −130·9 | 26·8 E | ... | ... | ... |
| 69·7 | 31·4 E | +0·63 | −133 | 0·256 |
| 54·6 | 31·4 E | +0·74 | −156 | 0·241 |
| 39·4 | 31·4 E | +0·96 | −203 | 0·217 |
| 24·2 | 31·4 E | +1·20 | −253 | 0·054 |
| 11·6 | 31·4 E | +1·30 | −274 | 0·070 |
| −1·1 | 31·4 E | +1·38 | −291 | 0·109 |
| −13·7 | 31·4 E | +1·87 | −395 | 0·202 |
| −26·4 | 31·4 E | +1·88 | −397 | 0·233 |
| −51·7 | 31·4 E | +2·49 | −525 | 0·093 |
| 73·1 | 35·8 E | +0·67 | −141 | 0·047 |
| 58·0 | 35·8 E | +1·02 | −215 | 0·085 |
| 42·8 | 35·8 E | (+0·90) | (−190) | (0·163) |
| | | +0·97 | −205 | 0·101 |
| 27·7 | 35·8 E | ... | ... | ... |
| 15·0 | 35·8 E | ... | ... | ... |
| 2·4 | 35·8 E | +1·37 | −289 | 0·101 |
| −10·3 | 35·8 E | +1·38 | −291 | 0·085 |
| −33·2 | 35·8 E | +1·82 | −384 | 0·093 |
| −48·2 | 35·8 E | +2·49 | −525 | 0·054 |
| 80·1 | 44·7 E | +0·67 | −141 | 0·054 |
| 68·0 | 44·7 E | ... | ... | ... |
| 49·8 | 44·7 E | (+0·90) | (−190) | (0·109) |
| | | ... | ... | ... |
| 9·3 | 44·7 E | +1·37 | −289 | 0·078 |
| −3·3 | 44·7 E | ... | ... | ... |
| −15·9 | 44·7 E | +1·82 | −384 | 0·054 |
| −41·2 | 44·7 E | ... | ... | ... |

TABLE I (*continued*)

| *Y* | *X* | Frequency displacement (Mc/s) | Velocity (km/s) | $N_H$ ($10^{21}$ cm$^{-2}$) |
|---|---|---|---|---|
| 87·0 | 53·7 E | ... | ... | ... |
| 56·7 | 53·7 E | (+0·97) | (−205) | (0·062) |
| | | ... | ... | ... |
| 3·6 | 53·7 E | ... | ... | ... |
| −9·0 | 53·7 E | ... | ... | ... |
| 148·2 | 4·5 W | +0·36 | −76 | 0·078 |
| 110·3 | 4·5 W | (+0·36) | (−76) | (0·078) |
| | | +0·30 | −63 | 0·124 |
| 42·0 | 4·5 W | +0·46 | −97 | 1·78 |
| 26·9 | 4·5 W | +0·73 | −154 | 1·31 |
| 11·7 | 4·5 W | +1·15 | −243 | 0·504 |
| −3·5 | 4·5 W | +1·40 | −295 | 0·481 |
| −16·1 | 4·5 W | (+1·62) | (−342) | (0·729) |
| | | +1·68 | −354 | 0·954 |
| −28·8 | 4·5 W | (+1·79) | (−378) | (0·722) |
| | | +1·98 | −418 | 1·16 |
| −41·4 | 4·5 W | +2·37 | −500 | 1·18 |
| −54·0 | 4·5 W | +2·43 | −513 | 0·745 |
| −79·3 | 4·5 W | +2·42 | −511 | 0·334 |
| −117·3 | 4·5 W | +2·37 | −500 | 0·629 |
| −155·2 | 4·5 W | ... | ... | ... |
| 144·8 | 8·9 W | +0·35 | −74 | 0·062 |
| 106·9 | 8·9 W | +0·36 | −76 | 0·109 |
| 38·6 | 8·9 W | +0·54 | −114 | 1·88 |
| 23·5 | 8·9 W | +0·77 | −162 | 1·37 |
| 8·3 | 8·9 W | +1·27 | −268 | 0·784 |
| −6·9 | 8·9 W | +1·48 | −312 | 0·598 |
| −19·5 | 8·9 W | +1·67 | −352 | 0·854 |
| −32·2 | 8·9 W | (+1·86) | (−392) | (0·947) |
| | | +1·96 | −414 | 1·23 |
| −44·8 | 8·9 W | +2·35 | −496 | 1·02 |
| −57·5 | 8·9 W | +2·46 | −519 | 0·714 |
| −82·8 | 8·9 W | +2·44 | −515 | 0·287 |
| −120·7 | 8·9 W | +2·36 | −498 | 0·427 |
| −158·6 | 8·9 W | ... | ... | ... |
| 141·3 | 13·5 W | +0·56 | −118 | 0·163 |
| 103·4 | 13·5 W | +0·56 | −118 | 0·132 |
| 35·1 | 13·5 W | +0·66 | −139 | 1·76 |
| 20·0 | 13·5 W | +0·96 | −203 | 1·28 |
| 4·8 | 13·5 W | +1·34 | −283 | 0·838 |
| −10·4 | 13·5 W | +1·46 | −308 | 0·698 |
| −23·0 | 13·5 W | (+1·63) | (−344) | (0·807) |
| | | +1·67 | −352 | 0·939 |
| −35·7 | 13·5 W | (+1·85) | (−390) | (0·768) |
| | | +1·98 | −418 | 1·10 |
| −48·3 | 13·5 W | +2·32 | −490 | 0·861 |
| −60·9 | 13·5 W | +2·46 | −519 | 0·388 |
| −86·2 | 13·5 W | +2·37 | −500 | 0·303 |
| −124·2 | 13·5 W | +2·43 | −513 | 0·256 |
| −162·1 | 13·5 W | ... | ... | ... |
| 139·2 | 16·2 W | +0·56 | −118 | 0·140 |
| 101·2 | 16·2 W | +0·35 | −76 | 0·054 |
| 32·9 | 16·2 W | +0·75 | −158 | 1·61 |
| 17·8 | 16·2 W | +0·90 | −190 | 1·16 |

TABLE I (*continued*)

| *Y* | *X* | Frequency displacement (Mc/s) | Velocity (km/s) | $N_H$ ($10^{21}$ cm$^{-2}$) |
|---|---|---|---|---|
| −12·5 | 16·2 W | +1·48 | −312 | 0·706 |
| −25·2 | 16·2 W | +1·53 | −323 | 0·792 |
| −37·8 | 16·2 W | (+1·90) | (−401) | (0·745) |
| | | +2·00 | −422 | 1·01 |
| −50·5 | 16·2 W | +2·31 | −487 | 0·799 |
| −63·1 | 16·2 W | +2·45 | −517 | 0·419 |
| −88·4 | 16·2 W | +2·38 | −502 | 0·279 |
| −126·3 | 16·2 W | +2·42 | −511 | 0·155 |
| −164·2 | 16·2 W | +2·16 | −456 | 0·039 |
| 136·5 | 19·6 W | +0·46 | −97 | 0·085 |
| 98·6 | 19·6 W | +0·36 | −76 | 0·062 |
| 30·3 | 19·6 W | +0·89 | −188 | 1·14 |
| 15·2 | 19·6 W | +1·14 | −241 | 1·02 |
| 0·0 | 19·6 W | +1·38 | −291 | 0·683 |
| −15·2 | 19·6 W | +1·50 | −317 | 0·504 |
| −27·8 | 19·6 W | +1·62 | −342 | 0·667 |
| −40·5 | 19·6 W | (+1·80) | (−380) | (0·442) |
| | | +1·89 | −399 | 0·636 |
| −53·1 | 19·6 W | +2·33 | −492 | 0·450 |
| −65·7 | 19·6 W | +2·55 | −538 | 0·202 |
| −91·0 | 19·6 W | +2·42 | −511 | 0·202 |
| −128·9 | 19·6 W | +2·36 | −498 | 0·085 |
| −166·9 | 19·6 W | ... | ... | ... |
| 133·7 | 23·3 W | +0·56 | −118 | 0·132 |
| 95·8 | 23·3 W | +0·36 | −76 | 0·039 |
| 27·5 | 23·3 W | +0·91 | −192 | 0·861 |
| 12·4 | 23·3 W | +1·24 | −262 | 0·830 |
| −2·8 | 23·3 W | +1·42 | −300 | 0·450 |
| −18·0 | 23·3 W | +1·58 | −333 | 0·396 |
| −30·6 | 23·3 W | +1·64 | −346 | 0·629 |
| −43·3 | 23·3 W | (+1·88) | (−397) | (0·334) |
| | | +1·95 | −411 | 0·427 |
| −55·9 | 23·3 W | +2·22 | −468 | 0·310 |
| −68·5 | 23·3 W | +2·65 | −559 | 0·171 |
| −93·8 | 23·3 W | +2·37 | −500 | 0·186 |
| −131·8 | 23·3 W | +2·36 | −498 | 0·039 |
| −169·7 | 23·3 W | +2·16 | −456 | 0·047 |
| 131·0 | 26·8 W | +0·48 | −101 | 0·093 |
| 93·0 | 26·8 W | ... | ... | ... |
| 24·8 | 26·8 W | +0·89 | −188 | 0·667 |
| 9·6 | 26·8 W | 1·10 | −232 | 0·404 |
| −5·6 | 26·8 W | +1·42 | −300 | 0·341 |
| −20·7 | 26·8 W | +1·65 | −348 | 0·233 |
| −33·4 | 26·8 W | 1·63 | −344 | 0·396 |
| −46·0 | 26·8 W | (+1·88) | (−397) | (0·241) |
| | | +1·99 | −420 | 0·349 |
| −58·7 | 26·8 W | +2·26 | −477 | 0·194 |
| −71·3 | 26·8 W | +2·65 | −559 | 0·178 |
| −96·6 | 26·8 W | +2·36 | −498 | 0·116 |
| −134·5 | 26·8 W | ... | ... | ... |
| −172·4 | 26·8 W | +2·16 | −456 | 0·039 |
| 127·5 | 31·4 W | +0·46 | −97 | 0·093 |
| 21·3 | 31·4 W | 0·62 | −131 | 0·341 |
| 6·2 | 31·4 W | (+1·50) | (−317) | (0·078) |
| | | +1·04 | −219 | 0·186 |

TABLE I (*continued*)

| $Y$ | $X$ | Frequency displacement (Mc/s) | Velocity (km/s) | $N_H$ ($10^{21}$ cm$^{-2}$) |
|---|---|---|---|---|
| −9·0 | 31·4 W | +1·29 | −272 | 0·155 |
| −24·2 | 31·4 W | +1·28 | 270 | 0·054 |
| −36·8 | 31·4 W | +1·55 | −327 | 0·295 |
| −49·5 | 31·4 W | (+1·82) | (−384) | (0·225) |
| | | +1·84 | −388 | 0·264 |
| −62·1 | 31·4 W | +2·35 | −496 | 0·047 |
| −74·8 | 31·4 W | ... | ... | ... |
| −100·1 | 31·4 W | +2·33 | −442 | 0·101 |
| −175·9 | 31·4 W | ... | ... | ... |
| 124·1 | 35·8 W | ... | ... | ... |
| 17·8 | 35·8 W | ... | ... | ... |
| 2·7 | 35·8 W | (+1·66) | (−350) | (0·147) |
| | | +1·44 | −304 | 0·264 |
| −12·5 | 35·8 W | +1·20 | −253 | 0·039 |
| −27·6 | 35·8 W | ... | ... | ... |
| −40·3 | 35·8 W | +1·61 | −340 | 0·217 |
| −52·9 | 35·8 W | +1·93 | −407 | 0·054 |
| −65·6 | 35·8 W | ... | ... | ... |
| −103·5 | 35·8 W | ... | ... | ... |
| −117·1 | 44·7 W | +0·56 | −118 | 0·039 |
| −4·2 | 44·7 W | +1·50 | −317 | 0·093 |
| −19·4 | 44·7 W | ... | ... | ... |
| −47·2 | 44·7 W | ... | ... | ... |
| −59·9 | 44·7 W | ... | ... | ... |
| 110·2 | 53·7 W | ... | ... | ... |
| −11·1 | 53·7 W | ... | ... | ... |

* Data from incomplete observations.
( ) A possible but less likely interpretation of the spectra.
... $T_B$ less than 0·5 °K.
$Y$, Distance measured northward along major axis; $X$, distance east or west along minor axis.

4. *Discussion of the drift scans and spectra.* Many of the drift scans in the declination interval ±40′ from the centre show structure comparable in size to the beamwidth. For example at +36′ drifts at various frequencies indicate the presence of features with half power widths estimated to be ∼13′ and steep edges rising to a maximum in ∼10′. These would correspond to linear dimensions projected on to the plane of the sky of 2·4 and 1·8 kpc at the adopted distance of 630 kpc (Baade 1963). Also some of the observed spectra in this same declination interval are not much wider than the bandwidth and indicate structure ∼200 kc/s in width. On the assumption that these values actually represent the magnitude of the angular and frequency structure the maximum brightness temperatures in M 31 would seem to be ∼20 °K and would indicate that these large areas are not optically thick if the kinetic temperature is taken to be ∼100 °K. Subsequent measurements with a 50 kc/s bandwidth support this conclusion although indicating that in some regions $T_B$ may be as high as 30 °K.

5. *The neutral hydrogen distribution in M 31.* The distribution of neutral hydrogen in M 31 can be obtained by integrating the spectra constructed every half beamwidth at each declination using the relation that the total number of neutral hydrogen atoms per cm$^2$ in the line of sight is

$$N_H = 1{\cdot}84 \times 10^{13} \int_{-\infty}^{+\infty} T_B(v)dv \text{ cm}^{-2}$$

provided the gas is optically thin, otherwise this expression gives a lower limit to $N_H$.

It is necessary to take a value for the distance of M 31 in order to determine its total mass and other properties. A number of recent estimates of its distance modulus have been made ranging from $24{\cdot}0^m$ (Baade 1963) to $24{\cdot}20^m$ (Baade & Swope 1963) and $24{\cdot}60^m$ (Th. Schmidt 1957). The value of $24{\cdot}0^m$ corresponding to 630 kpc favoured by Baade (1963) will be used here.

As shown in the previous section the most dense areas resolvable with the 250 ft radio telescope have $T_B \sim 30$ °K and probably are optically thin when averaged over regions $\sim 2$ kpc in diameter. However, it is likely that in smaller areas of M 31 the neutral hydrogen may have appreciable optical depth ($\tau \sim 1$) as it is in clouds within our own Galaxy and consequently the estimates of $N_H$ should strictly be regarded as lower limits. The distribution of surface density of neutral hydrogen projected onto the sky obtained from the spectra has been plotted in Fig. 4. Contours drawn with broken lines in the northern part of M 31 represent a possible extrapolation across the region in which there were limited observations.

Fig. 4 shows a number of significant features, the most striking of which are the concentrations of neutral hydrogen on the major axis at a distance of about 50′ either side of the centre. This is evidently part of a broad ring-like maximum in the neutral hydrogen about 9 kpc from the centre which is also visible as a double peak in the minor axis direction although here the observed maximum temperature has been reduced by the 15′ beam. Neutral hydrogen is not uniformly distributed within this ring-like feature; it shows for example three significant concentrations in the region between 10′ and 40′ south of the minor axis. An analysis of the overall neutral hydrogen distribution showed that the mass lying between the central declination and 36′ north is 1·10 times the mass lying in the same declination range to the south; the relative accuracy of the mass determinations is believed to be less than this difference and suggests a significant asymmetry between the two halves of M 31.

The mean density of neutral hydrogen in the plane of M 31 can be estimated for the regions of maximum surface density if the thickness is assumed to be the value of 220 pc found for the solar neighbourhood which is at a similar distance from the centre of the Milky Way system. For a surface density of $1{\cdot}5 \times 10^{21}$ cm$^{-2}$ which is the mean of the peak values in the north and the south of M 31, the mean density is 0·55 cm$^{-3}$ estimated on the basis of an inclination of the plane of the nebula of 14·5° to the line of sight (see van de Hulst, Raimond & van Woerden 1957). This value of the mean density averaged over an area 3 kpc in diameter may be compared with a comparable mean value of 0·7 cm$^{-3}$ for the arm and interarm regions in the solar neighbourhood of the Milky Way (Westerhout 1957). The density in the local spiral arm is $\sim 1{\cdot}2$ cm$^{-3}$.

The neutral hydrogen mass of M 31 can be calculated from the surface density distribution shown in Fig. 4 taking the interpolated distribution in the northern part of the nebula to represent the true distribution there. It was found to be $2{\cdot}4 \times 10^9$ solar masses and may be compared with $1{\cdot}4 \times 10^9$ solar masses in the Milky Way system (Westerhout 1958). The neutral hydrogen mass of M 31 calculated by Argyle (1965) from a complete survey of the nebula was $3{\cdot}1 \times 10^9$ solar masses corrected to a distance of 630 kpc which is consistent with the present result within the accuracy of the determinations. The above calculations

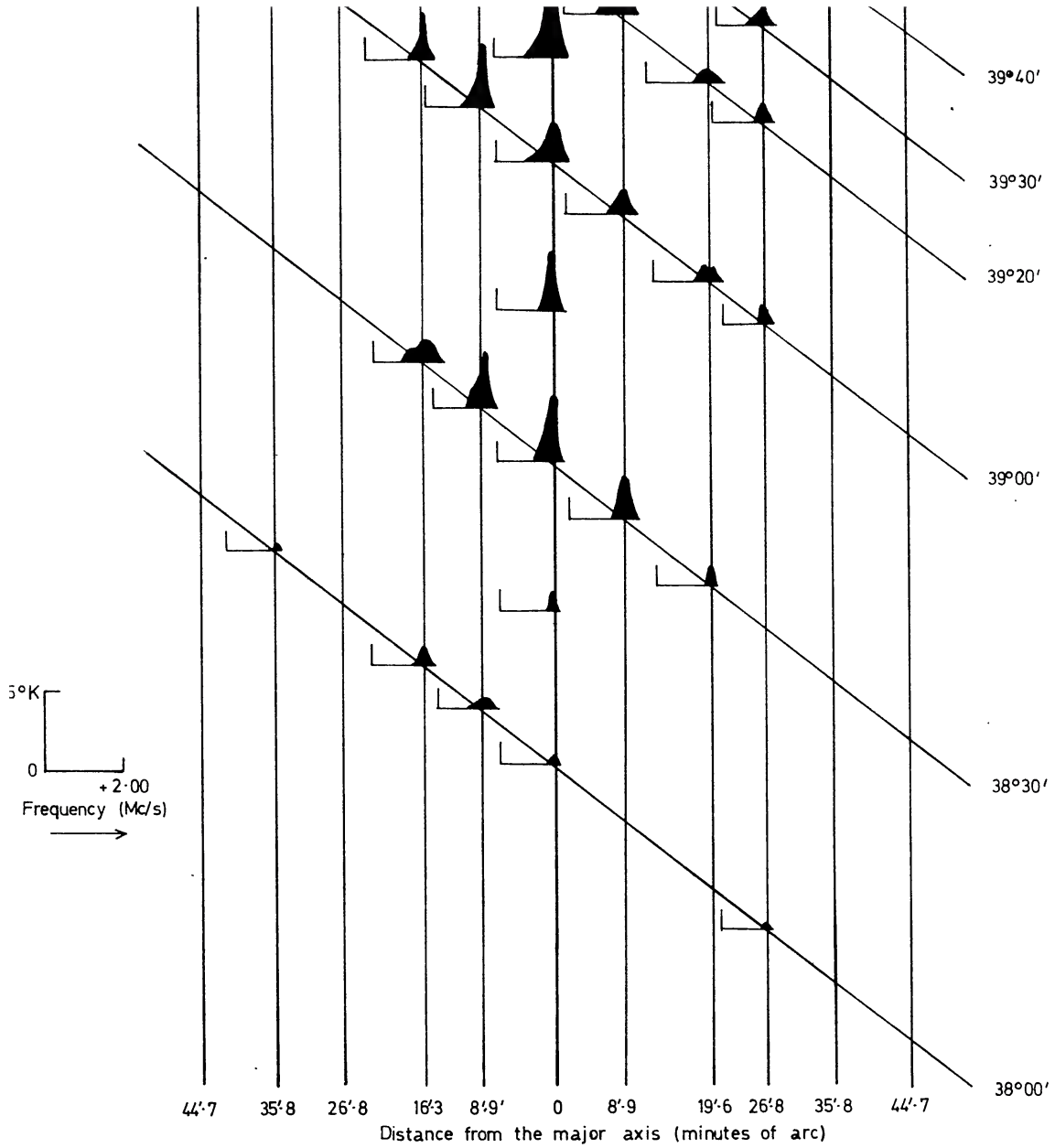


FIG. 3. *A summary of the spectral information obtained in the survey of M 31. The reference frequency on each spectrum is +1·00 Mc/s with respect to the l.s.r. Spectra are plotted such that the mean velocity coincides with the vertical axis.*

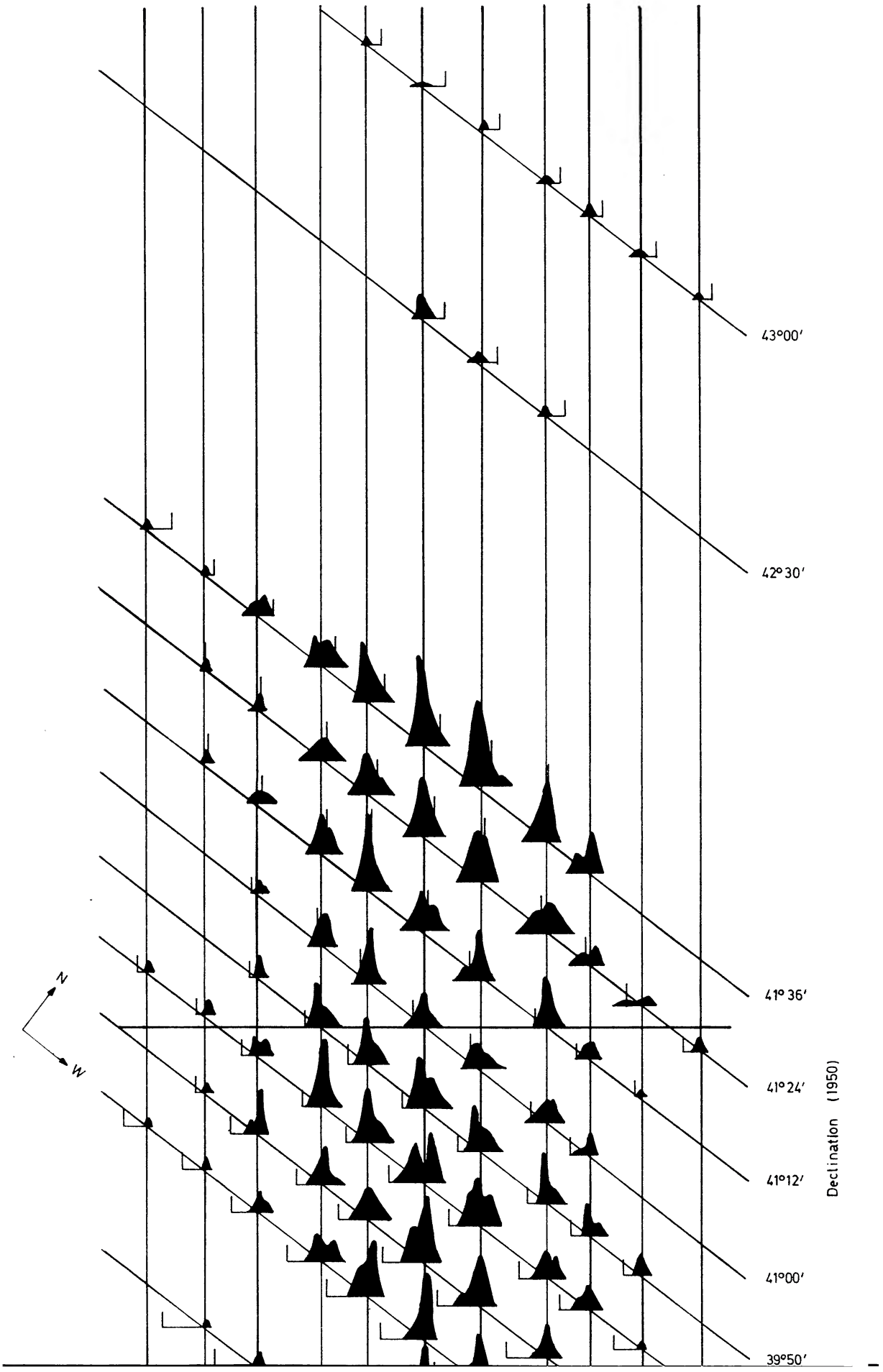

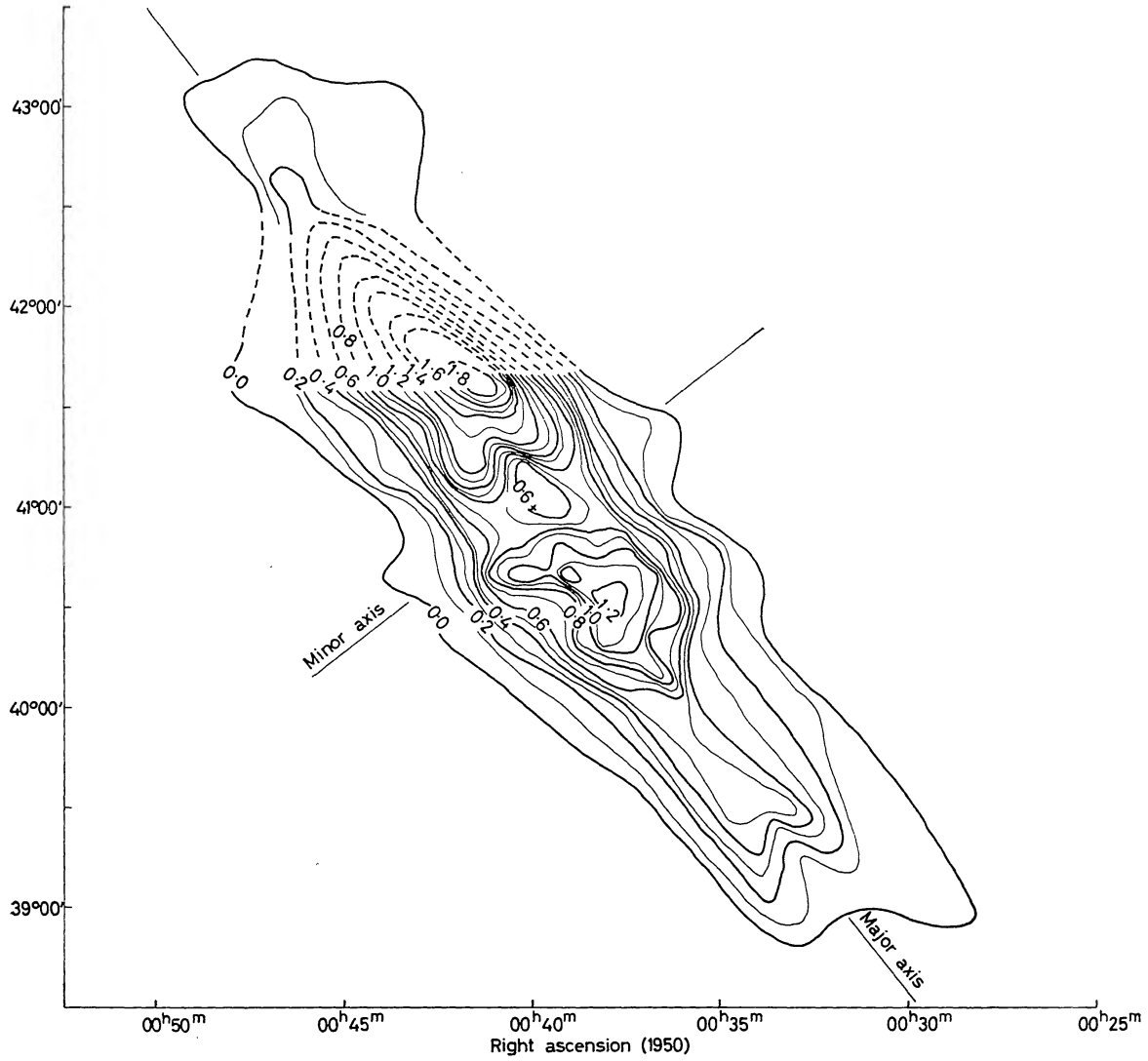


FIG. 4. *The distribution of surface density of neutral hydrogen projected into the plane of the sky. The contour interval is* $10^{21}$ *atoms* $cm^{-2}$.

assume as stated above that the gas is everywhere optically thin, but if the gas was concentrated into clouds of optical depth unity similar to that found in our own Galaxy (van Woerden & Takakubo 1960) the neutral hydrogen mass would have to be increased by $\sim 40\%$.

It is of interest to compare these values of the neutral hydrogen mass with an estimate of the ionized hydrogen masses of M 31 and the Milky Way system. Measurements of the continuum emission at 20 cm from M 31 (Kraus & Dixon 1965) show a peak brightness temperature of 0·20 °K falling to a value of 0·1 °K in a region 2° by 0·5° lying along the major axis. The thermal emission is likely to be confined within this area because the H II regions are concentrated here (Baade & Arp 1964). An upper limit to the ionized hydrogen emission can be derived from these observations by considering the spectrum of the continuum emission. Kenderdine & Baldwin (1965) have shown that the spectral index within this region is constant up to 20 cm wavelength with a value of $0{\cdot}53 \pm 0{\cdot}07$. If the non-thermal component has a curved spectrum similar to that inferred for the Milky Way system by Turtle (1963) then the thermal component in M 31

would have a brightness temperature of $\sim 0{\cdot}1$ °K at the centre. On the other hand if the non-thermal spectrum of M 31 is straight in the decimetre range as found by Wielebinski & Yates (1965) and by Komesaroff (1961) for the Milky Way system then the thermal component of M 31 will be less than 0·1 °K. An upper limit for the ionized hydrogen mass of M 31 was calculated using a brightness temperature of 0·1 °K extending over an area $2° \times 0{\cdot}5°$ and a layer thickness of 200 pc, the value found for the distribution of H II in the Milky Way. Assuming a uniform density of ionized hydrogen the upper limits of its mass is $3{\cdot}6 \times 10^8 M_\odot$. This corresponds to a value of $\sim 8{\cdot}4 \times 10^8 M_\odot$ calculated for the Milky Way from the data given by Westerhout (1958). More realistic values can be estimated on the basis that ionized hydrogen is concentrated in clouds with densities of typically $\sim 5\ \mathrm{cm}^{-3}$. (Westerhout 1958.) The ionized hydrogen content of M31 and the Milky Way then become $\leqslant 1{\cdot}5 \times 10^7 M_\odot$ and $8{\cdot}4 \times 10^7 M_\odot$ respectively. The ionized hydrogen content of M 31 is $\leqslant 0{\cdot}6\%$ of the neutral hydrogen compared with 6% in the Milky Way.

6. *A comparison of the optical and neutral hydrogen features of M* 31. The optical features of M 31 which lend themselves most readily to a comparison with the neutral hydrogen distribution are the spiral arms (Baade 1963) and the distribution of H II regions (Baade & Arp 1964). The distribution of neutral hydrogen along the major axis is given in Fig. 5 (*a*) which also includes the position at which the Baade spiral arms $N_1, \ldots, N_7$ and $S_1, \ldots, S_7$ intercept the major axis and the numbers of H II regions within $\pm 3'$ of the major axis in the various H II concentrations. The dashed curve in Fig. 5 (*a*) represents the observed neutral hydrogen distribution and the full-line curve is the result of a first order correction for beam smoothing. It can be seen immediately that the overall distribution of H II regions is similar to that of the neutral hydrogen in that each possesses a marked maximum in the region 30′ to 65′ from the centre. This also corresponds to the position of the major luminous spiral arms described by Arp (1964).

A detailed comparison of individual optical and neutral hydrogen features does not reveal a unique correspondence between them. Indeed the Baade arms and the H II regions are not coincident everywhere. In the SW end the neutral hydrogen surface density shows a feature at 20′ which has no spiral arm counterpart but which lies near the position of 3 H II regions slightly to the West of the major axis. This is perhaps the weakest correlation between a strong feature in the neutral hydrogen distribution and an optical feature. As will be discussed below it also appears as a distinct phenomenon in the major axis spectra in this region. The neutral hydrogen peak at 35′ corresponds to the H II concentration lying between the Baade arms S3 and S4 and the peak at 57′ corresponds to the H II regions lying immediately inside Baade arm S5. The neutral hydrogen maximum lying furthest out at 107′ would seem to be the unresolved counterpart of the smaller H II concentrations lying at the position of the Baade arms S6 and S7. A weak neutral hydrogen feature was detected at $\sim 145'$ along the southern major axis which is beyond the most outlying H II regions.

On the northern major axis there appear to be no neutral hydrogen or H II concentrations at the position of the Baade arms N1 and N2; the same lack of correlation was found for S1 and S2. However the marked change of slope at $\sim$ in the neutral hydrogen distribution corresponds to the clearcut H II concentrat associated with the arms N3. On the other hand the maximum in the north

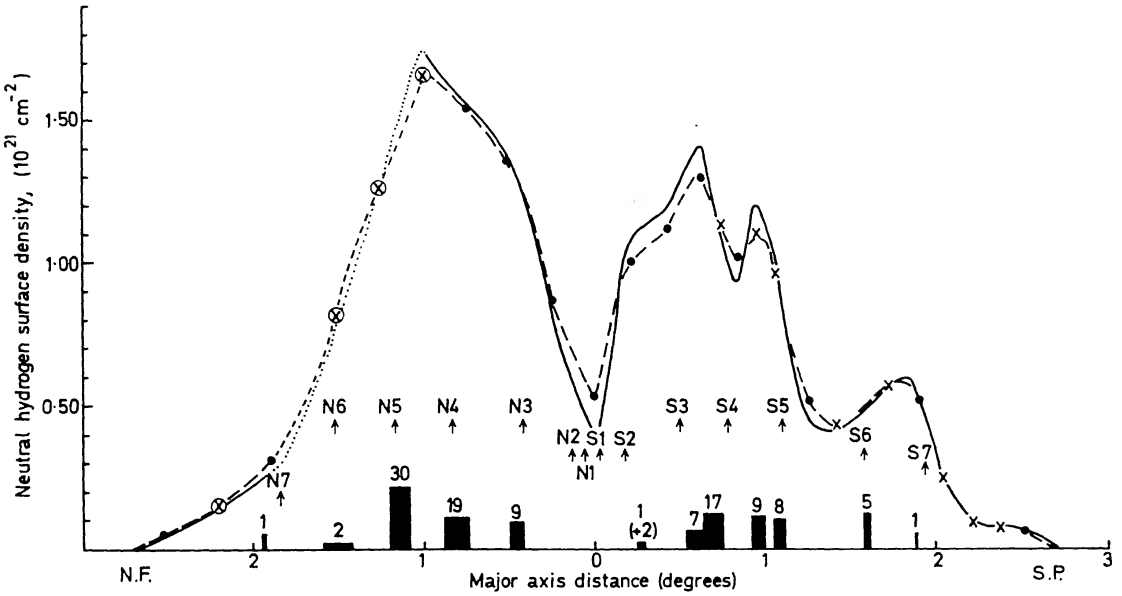


FIG. 5 (*a*). *The observed distribution of neutral hydrogen along the major axis of M* 31. *The full-line represents the distribution corrected for the beamwidth of the telescope.* (×) *Major axis scan data only;* (⊗) *limited observations. The major concentrations of H II regions (Arp & Baade* 1964) *within* ±3′ *of the major axis are also shown along with the number in each concentration. Baade spiral arms are indicated by arrows.*

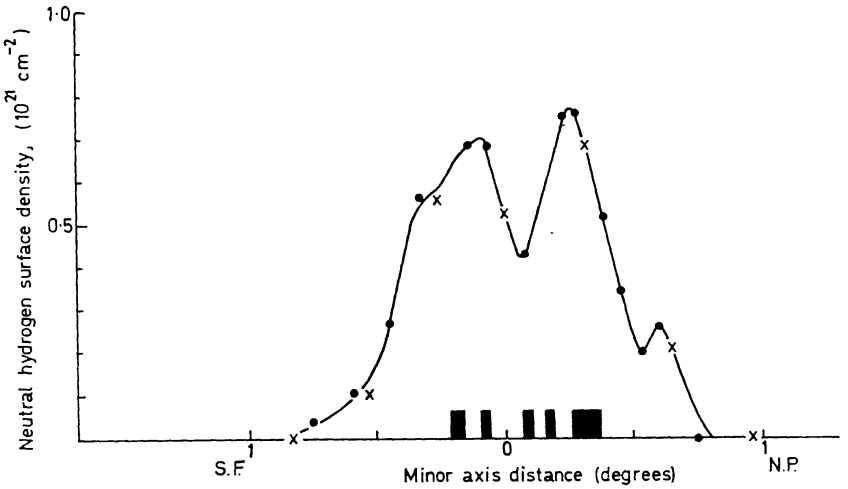


FIG. 5 (*b*). *The neutral hydrogen concentration along the minor axis of M* 31. *The major concentrations of H II regions (Arp & Baade* 1964) *are also shown.* (×) *Data obtained at points where R.A. scans crossed minor axis;* (●) *data obtained by interpolation from adjacent scans.*

63′ lies midway between the H II concentrations associated with the Baade arms N4 and N5. It must be remembered that the neutral hydrogen data becomes more scanty in the interval 63′ to 110′ and consequently detailed correlations should not be sought in this range, which includes the Baade arms N5, N6 and N7. As in the southern region neutral hydrogen appears to exist beyond the outer spiral arms.

The spectra with double peaks seen in Fig. 3 on the major axis at declination 10′, 20′ and 30′ south of the centre indicate the presence of two concentrations in the beam at each position which might suggest the presence of two neutral hydrogen spiral arms in this region of M 31. The major axis distribution in Fig. 5 (*a*) confirms such a picture. Circular spiral arms cutting the major axis

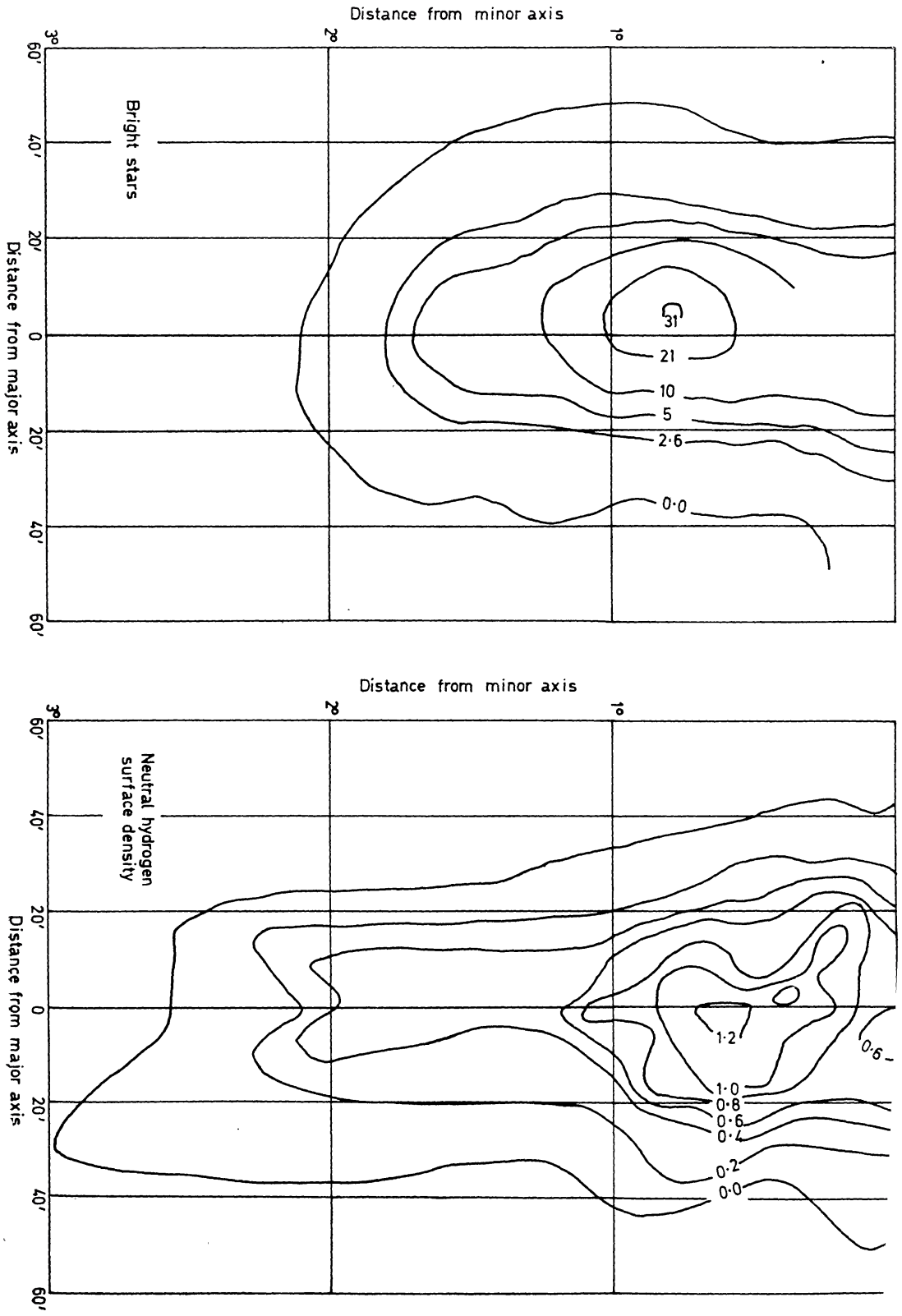


FIG. 6(*a*). *The distribution of neutral hydrogen and blue stars brighter than* $M_{pg} \sim -4{\cdot}5$ *in the southern part of M* 31 *smoothed with a* 15′ *beam. The neutral hydrogen contours are given in units of* $10^{21}$ *atoms* $cm^{-2}$ *and the blue contour star unit is bright stars per square minute. The stellar data is not corrected for obscuration.*

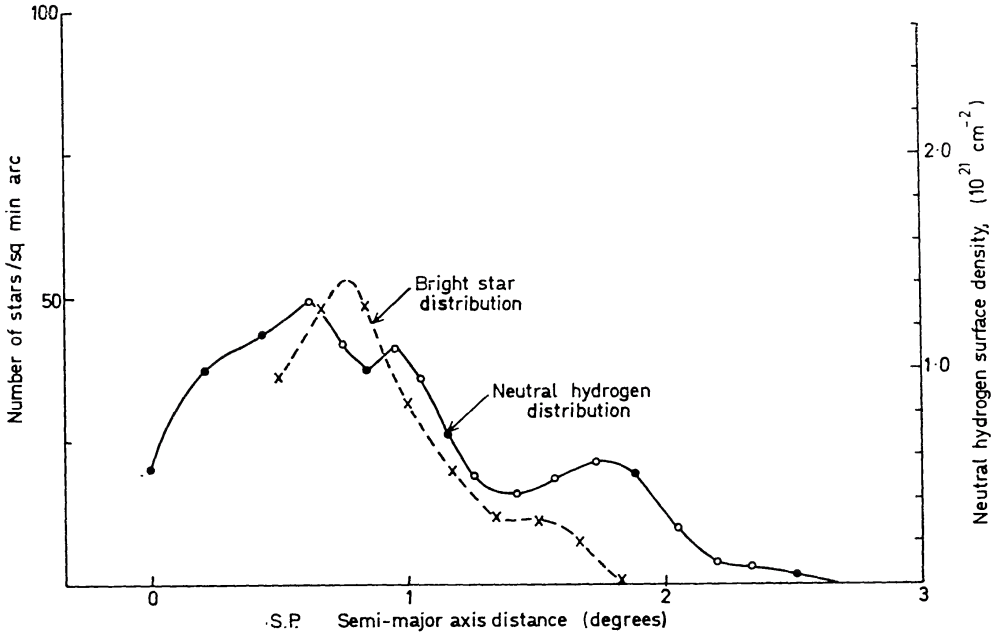


FIG. 6 (*b*). *The major axis distribution of neutral hydrogen and bright blue stars smoothed with a 15′ beam and corrected for obscuration.*

at 20′ and 35′ from the centre and having velocities taken from the rotation curve of Fig. 8 (*a*) would give spectra similar to those observed when scanned with a 15′ beam.

The minor axis distribution shown in Fig. 5 (*b*) has a similar minimum to that seen in the major axis distribution. However, because of the inclination of M 31 the angular resolution of the radio survey is not sufficient to separate the individual spiral arms. Nevertheless some structure is visible in the distribution and there is an indication of weaker features 30′ from the centre which may possibly be connected with similar structure seen at 120′ from the centre on the major axis distribution.

Another comparison between optical and neutral hydrogen distributions was made using a survey of bright blue stars corresponding to $M_{pg} \leqslant -4{\cdot}5$ published by Reddish (1962) for the southern regions of M 31. This survey has been smoothed with a 15′ beam for comparison with the neutral hydrogen distribution in Fig. 6 (*a*). The blue stars show a peak 48′ along the major axis which appears to be significantly further from the centre than the neutral hydrogen concentration at 35′. The second maximum in the blue star major axis distribution corrected for obscuration as indicated by Reddish is shown in Fig. 6 (*b*) to be situated at the position of Baade arm S6 and appears displaced relative to the neutral hydrogen maximum. The figure also shows that neutral hydrogen is distributed further from the centre than are the blue stars. In summary, it would appear that the neutral hydrogen shows a similar overall distribution to that of the H II regions while the (inner) Baade spiral arms and the blue stars mapped by Reddish show a poorer correlation.

7. *The rotation curve of M 31.* A rotation curve has been constructed from the spectra derived for the major axis of M 31 in the following way. The mean velocity of the neutral hydrogen at each point along the major axis was first

calculated from the observed data. Then because the non-uniform density influences the spectra observed with a 15′ beam a correction was made for this effect which was found to be never more than 20 km/s. The rotation curve corrected for this effect but not for the 14·5° inclination of the nebula is shown in Fig. 7. The rotation velocities corrected for inclination are given in Table II. The accuracy of specifying the mean frequency of the more intense spectra is believed to be ± 10 km/s, while the uncertainty in the weaker spectra is rather greater.

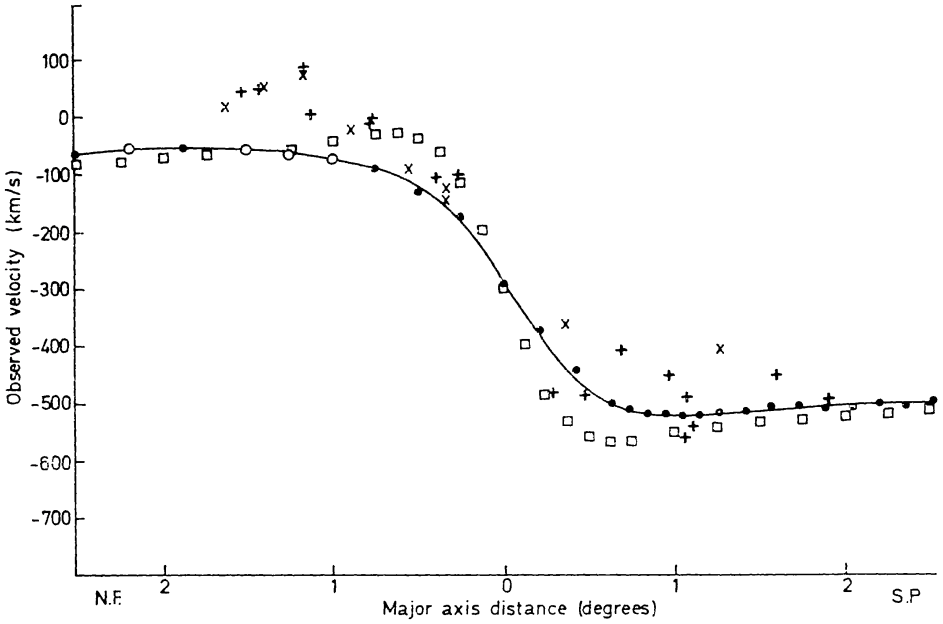


FIG. 7. *The observed rotation curve for M 31 corrected for the resolution of the 15′ beamshape.* (●) *Jodrell Bank data;* (○) *Jodrell Bank data from limited observations;* (□) *Leiden data as corrected for a 36′ beamshape by van de Hulst, Raimond & van Woerden;* (+) *optical velocities (Mayall 1950) for points lying near the major axis;* (×) *optical velocities for points lying more than 6′ from the major axis.*

It is evident that the present rotation curve is significantly different from that derived by the Leiden observers from their survey with the larger 36′ beam. A direct comparison between the present data and the rotation curve derived by Burke, Turner & Tuve was not possible because no errors were assigned to their curve, but an examination of their published spectral information gave a rotation curve not significantly different from the present one. It is also of interest to note that the published values of velocity derived from H II regions by Mayall (1950) are systematically higher than the neutral hydrogen values. The source of this difference is not clear, although a correction to the optical values may be necessary (Brandt 1960).

The difference in the shape of the derived rotation curve for the NE and SW sections is illustrated in Fig. 8 (*a*) where the curve has been reflected about a central velocity to give the best fit over the whole of the rotation curve. Despite this fitting of the rotation curve as a whole there are significant differences between the NE and SW sections of the rotation curve. The SW part has larger velocities between 30′ and 60′ than the NE part. These differences of the order of 25 km/s are thought to be real and have been checked on a preliminary analysis of the more recent 50 kc/s bandwidth data. Similar differences are seen in the section from

TABLE II

*Velocities of neutral hydrogen along the major axis of M 31*

| $Y$ (′) | $V$ rot. (km/s) | $Y$ (′) | $V$ rot. (km/s) |
|---|---|---|---|
| 151·7 | 234 | −50·6 | −231 |
| 132·7* | 243 | −56·9 | −232 |
| 113·4 | 245 | −63·2 | −236 |
| 91·0* | 239 | −69·5 | −236 |
| 75·8* | 234 | −75·8 | −232 |
| 60·7* | 224 | −85·3 | −228 |
| 45·5 | 208 | −94·8 | −221 |
| 30·4 | 166 | −104·3 | −217 |
| 15·2 | 123 | −113·8 | −223 |
| 0·0 | 0 | −123·3 | −221 |
| −12·6 | −80 | −132·7 | −215 |
| −25·3 | −156 | −142·2 | −217 |
| −37·9 | −215 | −151·7 | −213 |
| −44·3 | −225 | | |

The values have been corrected for instrumental effects, an inclination of 14°·5 to the line of sight and a systematic velocity of −289 km/s.

* Positions at which only limited data available.

80′ to 150′ but their reality is uncertain. The rotation curve obtained by Burke, Turner & Tuve shows asymmetries in the same sense as those indicated above. The difference between the NE and SW parts of the curve at distances less than 20′ from the centre is not significant in the present data because of the steep rise in density and velocity in this region and also because of the uncertainty of ±3′ in telescope positioning in this survey.

Further information which can be used to confirm the overall shape of the rotation curve was derived from spectra taken on axes inclined at ±10° to the major axis. The new points which are essentially independent of the major axis points beyond 60′ from the centre are shown in Fig. 8 (*b*) and are compared with major axis rotation curve scaled to a 10° position angle. These points differ from the major axis rotation curve in several regions and suggest the possibility that the rotation curve is not circularly symmetrical even between axes inclined at 35° in the plane of M 31. An asymmetrical distribution of neutral hydrogen could lead to similar observational differences. More detailed observations are required to establish this trend definitely.

The centre velocity of the rotation curve and thus the recession velocity of the nebula can be determined from the rotation curve of Figs. 7 and 8 (*b*) in several ways using different criteria. Firstly, the velocity about which the SW part of the rotation curve is reflected to give the best overall fit to the NE part for hydrogen at less than 70′ from the centre is −290 km/s. Secondly, if the fit is made for hydrogen more than 40′ from the centre the velocity is −283 km/s. On the other hand if all the data from the rotation curves obtained along axes inclined ±10° to the major axis is used then the velocity is −295 km/s. The mean value of these velocities, −289 ± 5 km/s, is representative of a wide distribution of rotational data over M 31 and probably gives the best estimate of its recession velocity from the present observations. This may be compared with −296 ± 3 km/s obtained by van de Hulst, Raimond & van Woerden by taking the mean velocity of a series of points on opposite sides of the centre of the nebula. The

mean velocity of all the neutral hydrogen in M 31 was found by Argyle to be $-295 \pm 0{\cdot}4$ km/s. This estimate does not give the true recession velocity of the nebula and will not agree with those derived from the rotation curve unless the neutral hydrogen distribution is circularly symmetrical which is apparently not the case.

8. *The mass distribution in M 31.* The total mass of all matter and the distribution of mass in the nebula can be derived from the rotation curve of Fig. 7. The

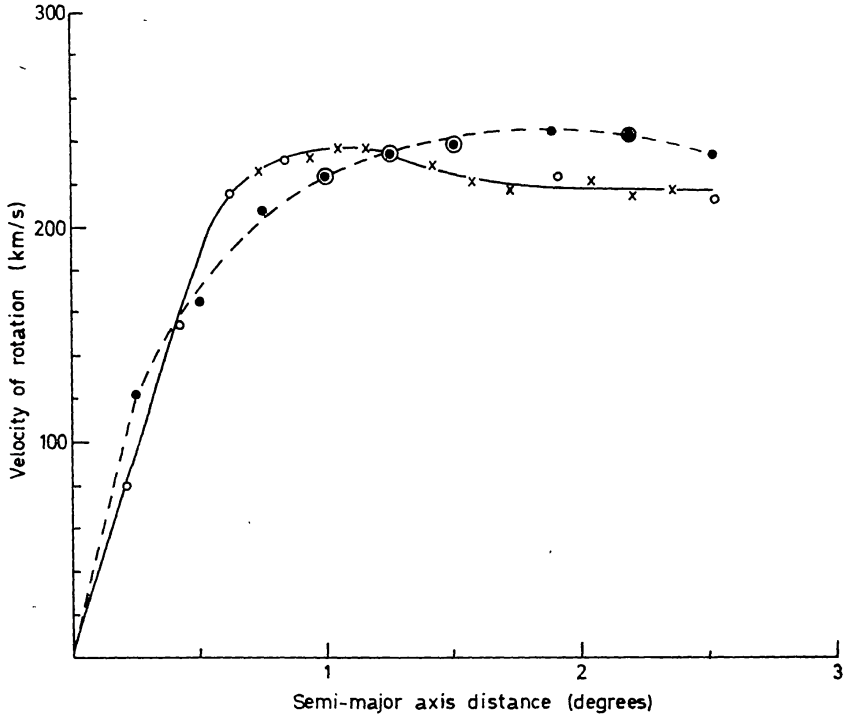


FIG. 8 (*a*). *A comparison of the NE and SW rotation curves of M 31 corrected for the 14·5° inclination of the plane of the nebula to the line of sight.* (○) *SW data from drift curves;* (×) *SW data from major axis scans;* (•) *NE data from drift curves;* ⊙ *NE incomplete data.*

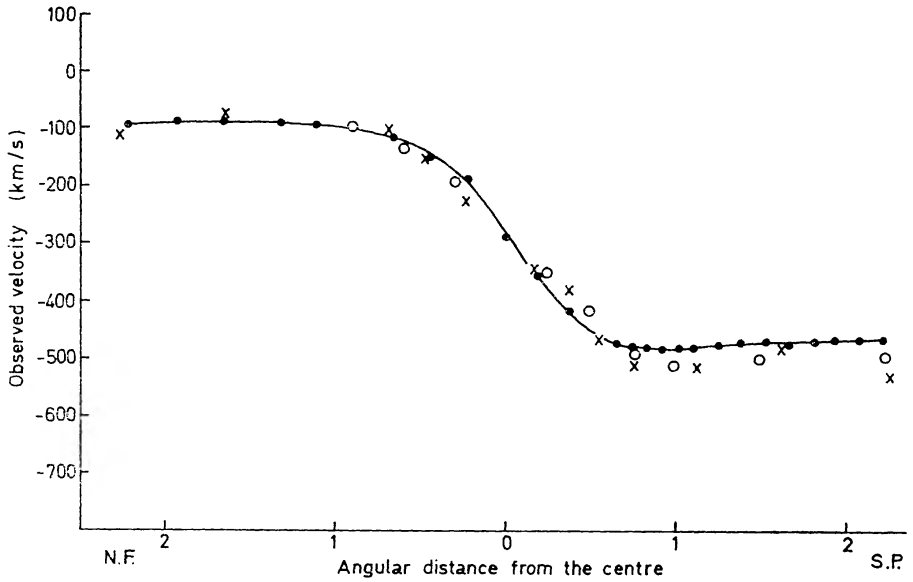


FIG. 8 (*b*). *The major axis rotation curve scaled for direct comparison with rotation curves obtained along axes inclined at +10° and −10° to the major axis.* (●) *Predicted values from major axis points;* (○) *observations at position angle +10°;* (×) *observations at position angle −10°.*

rotation curve could be fitted within the accuracy of the measurements to one of the analytical functions discussed in detail by Brandt (1960) and Brandt & Belton (1962). The best fit was found to the rotation curve in which the circular velocity $V$ varied with distance $\tilde{\omega}$ from the centre as

$$V(\tilde{\omega}) = \frac{U\tilde{\omega}}{1+(B\tilde{\omega})^{3/2}}$$

where $U$ and $B$ are parameters related to the velocity, $V_{max}$, and the position, $\tilde{\omega}_{max}$, of the turnover point of the rotation curve. Using the values of $V_{max}$ and $\tilde{\omega}_{max}$ of the analytical curve of the form shown which best fits the observed points the mass distribution was evaluated following the calculations of Brandt & Belton. The NE and SW parts of the rotation curve and the mean rotation curve were used separately to evaluate firstly the mass within a cylindrical section through M 31 with a radius of 150′ which corresponds to the limit of observations and secondly the total mass derived from the analytical rotation curve taken to large distances. The results which are given in Table II for a distance of 630 kpc have been increased by 10% (Brandt 1960) to allow for an assumed axial ratio of 0·08 typical of spiral galaxies. The mass within 150′ from the centre obtained from the various rotation curves has a consistent value of $\sim 2{\cdot}4 \times 10^{11} M_{\odot}$. This may be compared with a value of $2{\cdot}4 \times 10^{11} M_{\odot}$ out to 120′ derived for the NE rotation curve by Burke, Turner & Tuve (1964). However the values given in Table III for the total mass of $\sim 5 \times 10^{11} M_{\odot}$ are probably not very accurate since no observations are available from any source for the outer regions of M 31, and the mass distribution here is of necessity derived from the adopted model rotation curve. For example with the present model 25% of the mass lies beyond $5\tilde{\omega}_{max}$. Previous estimates of the mass (see Brandt 1906) range from 3·5 to $4{\cdot}0 \times 10^{11} M_{\odot}$ based on various analyses of older radio and optical rotation curves.

TABLE III

*Estimates of the mass of M 31*

| Rotation curve | $V_{max}$ (km/s) | $\varpi_{max}$ (′) | Mass to 150′ (solar masses) | Total mass (solar masses) |
|---|---|---|---|---|
| NE | 246 | 111 | $3{\cdot}0 \times 10^{11}$ | $7{\cdot}1 \times 10^{11}$ |
| SW | 235 | 69 | $2{\cdot}2 \times 10^{11}$ | $3{\cdot}9 \times 10^{11}$ |
| Mean | 237 | 82 | $2{\cdot}4 \times 10^{11}$ | $4{\cdot}8 \times 10^{11}$ |

The total mass distribution corresponding to the mean rotation curve is shown in Fig. 9 where it is compared with that obtained by Schmidt (1957) from the van de Hulst, Raimond & van Woerden data. The new rotation curve corresponds to a less sharp central concentration of total mass. The mean neutral hydrogen distribution along the major axis is also shown but on a scale reduced by 100 compared with the total mass distribution. It demonstrates the reduction in the fractional neutral hydrogen content inside a distance 60′ from the centre.

The mass composition of M 31 is summarized and compared with that of the Milky Way (Schmidt 1956) in Table IV. It can be seen that the fractional neutral hydrogen masses of M 31 and the Milky Way are similar (1–2%) within the accuracy of determining the total mass in each case. The largest difference

between the composition of the two systems appears to be in the calculated amounts of H II, with M 31 containing less than the Milky Way.

9. *The mass to luminosity ratio.* The mass distribution derived in the previous section can be used in conjunction with the blue luminosity distribution $L_B$

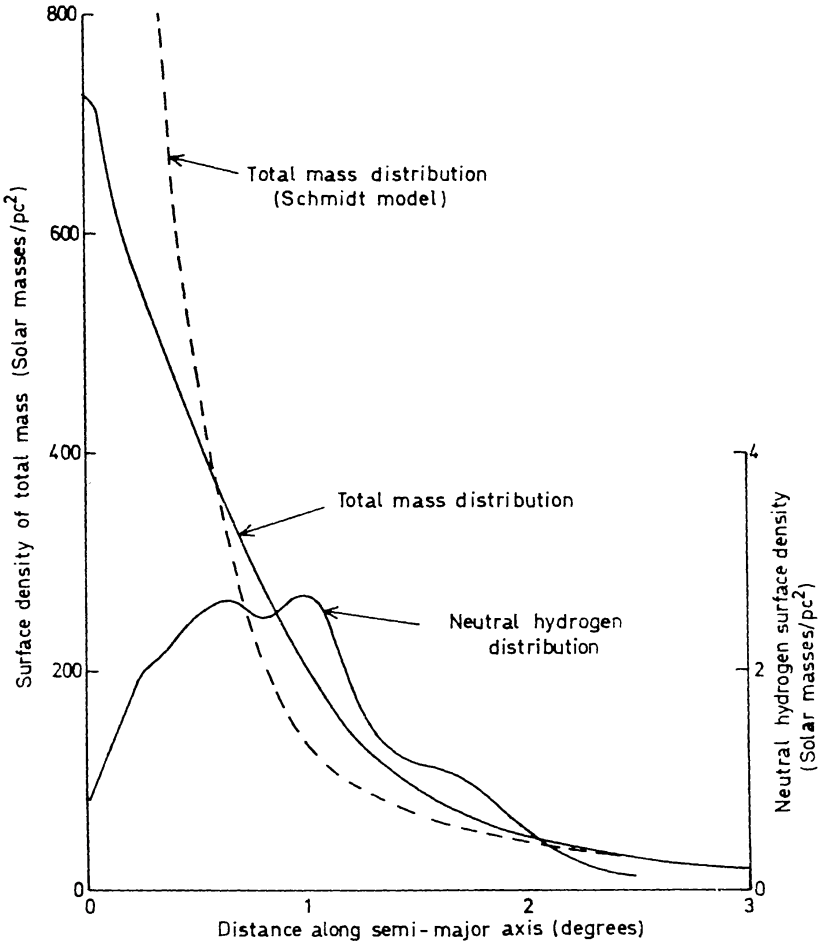


FIG. 9. *The distribution of total mass derived from the mean rotation curve compared with the neutral hydrogen distribution. The total mass distribution obtained by Schmidt* (1957) *from the van de Hulst, Raimond & van Woerden rotation curve is shown by the broken curve.*

TABLE IV

*Mass composition of M 31 and the Milky Way*

| Mass (solar masses) | M 31 | Milky Way |
|---|---|---|
| Total mass ($M_T$) | $4{\cdot}8 \times 10^{11}$ | $7 \times 10^{10}$* |
| Mass to 150′ ($M_{150'}$) | $2{\cdot}4 \times 10^{11}$ | — |
| H I mass ($M_{HI}$) | $2{\cdot}4 \times 10^{9}$ | $1{\cdot}4 \times 10^{9}$* |
| H II mass ($M_{HII}$) | $\leqslant 1{\cdot}5 \times 10^{7}$ | $8{\cdot}4 \times 10^{7}$* |
| $\frac{M_{HI}}{M_{150'}}$ | 0·010 | $\left(\frac{M_{HI}}{M_T} = 0{\cdot}020\right)$ |
| $\frac{M_{HII}}{M_{HI}}$ | $\leqslant$0·006 | 0·060 |

* These value are increased by a factor of 1·5 if the new IAU (1963) galactic rotation constants are used.

given by de Vaucouleurs (1958) to establish the variation of the $M/L_B$ ratio across M 31. The values of luminosity projected on to the sky and the axial ratio given in his Table 4 have been used to calculate the luminosity projected on to the equatorial plane and thence the values of $M/L_B$ in Table V. A significant feature of the variation of $M/L_B$ with distance from the centre is its constancy between 30′ and 75′ at a value of $\sim 20$. This is the region where the spiral structure dominates and has a uniform composition. In the outer regions beyond 75′ the $M/L_B$ ratio appears to gradually increase again. Since the NE and SW sections of the rotation curve show this effect independently the increase is believed to be real. Similar effects were noted by de Vaucouleurs (1958).

TABLE V

| Distance from centre (′) | Luminosity ($L_B$) $L_\odot$ pc$^{-2}$ | Mass density ($M$) $M_\odot$ pc$^{-2}$ | $M/L_B$ |
|---|---|---|---|
| 5·0 | 330 | 680 | 2·1 |
| 7·3 | 210 | 650 | 3·1 |
| 11·5 | 105 | 600 | 5·7 |
| 18·5 | 48 | 530 | 11 |
| 27·2 | 29 | 450 | 16 |
| 42·5 | 16·6 | 330 | 20 |
| 53 | 11·8 | 240 | 20 |
| 60·7 | 8·9 | 190 | 21 |
| 69 | 6·9 | 150 | 22 |
| 75 | 5·2 | 130 | 25 |
| 78·5 | 4·1 | 120 | 29 |
| 86 | 3·0 | 100 | 33 |
| 96·5 | 1·8 | 77 | 43 |
| 107·5 | 1·1 | 64 | 60 |

Inside 30′ the derived $M/L_B$ ratio falls to a value of about 2 at 5′ from the centre. The accuracy of this low value of $M/L_B$ in the central regions will now be discussed in detail. The values of $M$ used in deriving the $M/L_B$ distribution are those obtained from the analytical model which gives a best fit to all the observed points in the rotation curve. Since the observed values of rotation velocity within 30′ of the centre are 10% lower than those used in the model, the mass densities derived from the model would be about 20% high. Furthermore the mass density distribution derived from the northern and southern parts of the rotation curve are in agreement to within $\pm 12\%$ thus confirming the reality of the derived mass distribution and consequently the trend of values of $M/L_B$ in Table V.

The uncertainty in the observed rotation velocities in the central regions of M 31 will lead to an uncertainty in the derived mass. At 17′ from the centre for example the uncertainty in the velocity is $\pm 10$ km/s which corresponds to a mass uncertainty interior to 17′ of $\pm 17\%$. In addition there will be systematic errors in measuring the velocities in the inner regions of M 31 due to the non-uniform distribution of neutral hydrogen. The velocities shown in Fig. 8 (*a*) have already been corrected to account for this as explained in a previous section.

Systematic effects which might increase $M/L_B$ in the central regions will now be discussed. If the material inside 17′ had a more spherical distribution than the constant axial ratio of 0·08 taken in the model for the whole galaxy then its mass would be 36% greater. However the light distribution in this

region is substantially flattened with an axial ratio of about 0·4 and so the mass which is likely to be similarly distributed will not be increased by this percentage. Furthermore the $M/L_B$ distribution in Table V could be substantially altered by a systematic variation of obscuration along the major axis. De Vaucouleurs (1958) suggests that there might be such a variation ranging from $0{\cdot}6^m$ in the spiral arm regions to a smaller value inside 17·5′ of $0{\cdot}2^m$ as inferred from his data. This would produce an increase of $M/L_B$ in the central regions relative to the outer regions of 50%. However no accurate estimate has been made of the obscuration which is known to exist in the central areas. In might be considered that this systematic effect of 50% represents an upper limit to the increase in $M/L_B$.

If the two systematic effects are added the $M/L_B$ ratio inside 17′ could be doubled relative to the values given for the areas outside 30′ say. This maximum upwards correction still leaves the central regions with an $M/L_B$ less than half the value at the position of the developed spiral arms.

The value of $M/L_B$ obtained for the nebula as a whole using $M_T = 4{\cdot}8 \times 10^{11} M_\odot$ and $L_B = 1{\cdot}4 \times 10^{10} L_{B\odot}$ which corresponds to $M_{pg} = 4{\cdot}36$ at 630 kpc (de Vaucouleurs 1958) is 34. As $M_T$ is not accurately known a better determination of $M/L_B$ can be made out to a distance of 120′ where both $M$ and $L_B$ (derived from $B = 4{\cdot}39$) are determined directly from the observations. The corresponding value of $M/L_B$ is 16. These values can be corrected for obscuration within M 31, which is estimated as $0{\cdot}6^m$ by de Vaucouleurs, and are listed in Table VI.

TABLE VI

*Mass–luminosity ratios for M 31*

| | Mass (solar masses) | Luminosity on $B$ magnitude system (Suns) | $M/L_B$ | $M/L_B$ corrected for obscuration |
|---|---|---|---|---|
| Total | $4{\cdot}8 \times 10^{11}$ | $1{\cdot}40 \times 10^{10}$ | 34 | 19 |
| Out to 120′ | $2{\cdot}1 \times 10^{11}$ | $1{\cdot}36 \times 10^{10}$ | 16 | 9 |

10. *Conclusion.* The present study has outlined the distribution of neutral hydrogen in the Sb galaxy M 31. One feature of this distribution is the deficiency of neutral hydrogen within 3 kpc of the centre where the density falls to less than 30% of its value at 10 kpc. This corresponds to the region where there is a smaller fraction of other population I material in M 31. The major concentration of neutral hydrogen lies in a ring extending from 7 to 12 kpc from the centre and is assumed to be in the plane of the galaxy. This hydrogen is not uniformly spread throughout the ring but has several concentrations which are particularly clear south of the nucleus. Their masses are of the order of $5 \times 10^6 M_\odot$ and appear comparable in size with the neutral hydrogen complexes of $5\text{–}20 \times 10^6 M_\odot$ found by McGee (1964) in the developed arms of our own Galaxy. A 10% asymmetry was also found in the amount of neutral hydrogen out to declination 36′ north and south of the centre. This asymmetry will however produce no detectable dynamical effects in M 31 since it is equivalent to only 0·02% of the total mass.

A systematic difference was found between the NE and SW parts of the rotation curve which indicates the existence of large-scale departures from a circularly symmetrical rotation curve. Similar effects have been found by Burbidge, Burbidge & Prendergast (1962) in their optical studies of galaxies.

Such streaming motions may also be characteristic of the Milky Way as has been reported by Blaauw (1962) for a gas complex near $h$ and $\chi$ Persei.

The mass distribution derived from the observed rotation curve has been used to investigate the distribution of $M/L_B$ along the major axis of M 31. This distribution can be related to the distribution of different stellar populations along the major axis. In the region from 30′ to 75′ where $M/L_B$ has a constant value of 20 are found the major spiral arms containing young stars and numerous H II regions. Within 30′ of the centre $M/L_B$ falls rapidly and so also does the fraction of population I material. Beyond 75′ from the centre $M/L_B$ increases in a region of gradually falling density. The increase of $M/L_B$ at greater distances from the centre of M 31 could be interpreted as being due to an increase in the fraction of uncondensed material or in the fraction of lower luminosity stars at these distances.

The significant fall in the observed value of $M/L_B$ within 20′ of the centre of M 31 is of considerable interest, but before its astrophysical singificance is discussed a further source of uncertainty in the mass distribution in the central region of a galaxy should be mentioned. If substantial turbulent (non-gravitational) velocities exist these will result in an increase of the derived mass. However, in the case of M 31 any such upwards correction of the mass would appear to be small because the turbulent mass motions observed in the centremost gaseous regions (Münch 1960) and the neutral hydrogen spectra at 17′ from the centre are less than the observed rotational velocity at 17′ from the centre. For this reason and those given in the previous section the actual values of $M/L_B$ in Table V should be treated with caution although it is believed that there is a significant fall of $M/L_B$ towards the centre of M 31.

Studies of the $M/L$ ratio of galaxies of different morphological types show that irregular and Sc galaxies have smaller values of $M/L$ than Sb, Sc and elliptical galaxies (see for example Roberts 1963). The fall of $M/L$ in the regions of M 31 which contain the more evolved stars thus shows a trend opposite to that found for the more evolved galaxies. On the other hand the population II globular clusters characteristic of the galactic halo have values of $M/L < 1$ (Feast & Thackeray 1960, Hogg 1959) and it could be argued that the nuclear regions of galaxies have similar stellar contents to the globular clusters. Although the value of $M/L$ is similar, there is a significant spectroscopic difference between the nuclear regions of galaxies and halo globular clusters in that the former are more metal-rich than the latter. It is interesting to note that the concentrated nucleus of M 31 about 3″ arc in diameter also has a $M/L$ of about 3·6 (Lallemand, Duchesne & Walker 1960), but this region is several orders of magnitude smaller in extent than the regions of low $M/L$ found in the present study. The problem of interest which emerges is that the central evolved regions of a spiral galaxy like M 31 and the globular clusters of our own Galaxy should have a value of $M/L$ ten times smaller than the integrated $M/L$ for the (evolved) elliptical galaxies.

A marked difference found between M 31 and the Milky Way was the difference in the ratio of ionized to neutral hydrogen emission. On the basis of clouds of the same density in the two systems it was concluded that the ratio of the ionized to neutral hydrogen masses in M 31 was $\leqslant 0{\cdot}1$ of that in the Milky Way. Alternatively the difference in emission could be attributed to a lower density within the H II regions of M 31. The ratio of the ionized to neutral hydrogen masses would then be more nearly equal.

It is evident that more sensitive measurements using narrower bandwidths are required to investigate a number of problems raised in the present survey. Foremost are studies of the multiple peaked spectra in the central regions which could be used to determine the inner spiral structure and to examine any expansion of neutral hydrogen in the central regions. It would be also of interest to search for counterparts in the Andromeda nebula of the weak high velocity clouds seen at high latitudes in the Milky Way.

*Acknowledgments.* We wish to thank Dr G. L. Verschuur for assistance with the observations and Sir Bernard Lovell for his interest in this investigation. The contribution to the reduction of the extensive data by Mr H. Griffiths, Miss J. Ferguson and Miss S. K. Jones is acknowledged. Dr C. G. T. Haslam provided the computer programme for the convolution of the star map in Fig. 6.

One of us (S.T.G.) is grateful for a Fulbright Scholarship and a Junior Leverhulme Research Fellowship held during the period of this work.

*Nuffield Radio Astronomy Laboratories,*
*Jodrell Bank,*
*University of Manchester:*
1965 *October.*

## *References*

Argyle, E., 1965. *Astrophys. J.*, **141**, 750.
Arp, H., 1964. *Astrophys. J.*, **139**, 1045.
Baade, W., 1963. *Evolution of Stars and Galaxies*, p. 59. Harvard University Press.
Baade, W. & Swope, H. H., 1963. *Astr. J., N.Y.*, **68**, 435.
Baade, W. & Arp, H., 1964. *Astrophys. J.*, **139**, 1027.
Blaauw, A., 1962. *Interstellar Matter in Galaxies* (Ed. by L. Woltjer), p. 63. Benjamin New York.
Brandt, J. C., 1960. *Astrophys, J.*, **131**, 293.
Brandt, J. C. & Belton, M. J. S., 1962. *Astrophys. J.*, **136**, 352.
Burke, B. F., Turner, K. C. & Tuve, M. A., 1964. *Yb. Carnegie Instn Wash.*, No. 6; p. 341.
Feast, M. W. & Thackeray, A. D., 1960. *Mon. Not. R. astr. Soc.*, **120**, 463.
Hogg, H. S., 1959. *Handb. Phys.*, **53**, 129.
I.A.U., 1963. *Information Bulletin* No. 11, p. 10.
Kenderdine, S. & Baldwin, J. E., 1965. *Observatory*, **85**, 24.
Komesaroff, M. M., 1961. *Aust. J. Phys.*, **14**, 515.
Kraus, J. D. & Dixon, R. S., 1965. *Nature, Lond.*, **207**, 587.
Lallemand, A., Duchesne, M. & Walker, M. F., 1960. *Publs astr. Soc. Pacif.*, **72**, 76.
Mayall, N. U., 1950. *Publs Obs. Univ. Mich.*, **10**, 19.
McGee, R. X., 1964. *The Galaxy and the Magellanic Clouds*, IAU-URSI Symposiu No. 20 (Ed. by F. J. Kerr & A. W. Rodgers), p. 26. Australian Academy Science.
Muller, C. A. & Westerhout, G., 1957. *Bull. astr. Insts Neth.*, **13**, 151.
Münch, G., 1960. *Astrophys. J.*, **131**, 250.
Münch, G., 1964. IAU General Assembly, Hamburg, August 1964.
Reddish, V. C., 1962. *Z. Astrophys.*, **56**, 194.
Roberts, M. S., 1963. *A. Rev. Astr. Astrophys.*, **1**, 149.
Schmidt, M., 1956. *Bull. astr. Insts Neth.*, **13**, 15.
Schmidt, M., 1957. *Bull. astr. Insts Neth.*, **14**, 7.
Schmidt, Th., 1957. *Z. Astrophys.*, **41**, 197.

Turtle, A. J., 1963. *Mon. Not. R. astr. Soc.*, **126**, 405.
van de Hulst, H. C., Raimond, E. & van Woerden, H., 1957. *Bull. astr. Insts Neth.*, **14**, 1.
de Vaucouleurs, G., 1958. *Astrophys. J.*, **128**, 465.
Westerhout, G., 1957. *Bull. astr. Insts Neth.*, **13**, 201.
Westerhout, G., 1958. *Bull. astr. Insts Neth.*, **14**, 215.
Wielebinski, R. & Yates, K. W., 1965. *Nature, Lond.*, **205**, 581.
van Woerden, H. & Takakubo, K., 1960. *Present Problems Concerning the Structure and Evolution of the Galactic System*, pp. ix, 21. The Hague NUFFIC.